Visual and Nondestructive Evaluation Inspection of Live Gas Mains Using the Explorer™ Family of Pipe Robots

Hagen Schempf, Edward Mutschler, Alan Gavaert, George Skoptsov, and William Crowley
Carnegie Mellon University, The Robotics Institute, 5000 Forbes Avenue, Pittsburgh, Pennsylvania 15213
e-mail: hagen+@cmu.edu

Received 18 May 2009; accepted 3 November 2009

Visual inspection and nondestructive evaluation (NDE) of natural gas distribution mains is an important future maintenance cost-planning step for the nation's gas utilities. These data need to be gathered at an affordable cost with the fewest excavations and maximum linear feet inspected for each deployment, with minimal to no disruption in service. Current methods (sniffing, direct assessment) are either postleak reactive or too unreliable to offer a viable and Department of Transportation–acceptable approach as a whole. Toward achieving the above goal, a consortium of federal and commercial sponsors funded the development of Explorer™. Explorer™ is a long-range, untethered, self-powered, and wirelessly controlled modular inspection robot for the visual inspection and NDE of 6- and 8-in. natural gas distribution pipelines/mains. The robot is launched into the pipeline under live (pressurized flow) conditions and can negotiate diameter changes, 45- and 90-deg bends and tees, as well as inclined and vertical sections of the piping network. The modular design of the system allows it to be expanded to include additional inspection and/or repair tools. The range of the robot is an order of magnitude higher (thousands of feet) than present state-of-the-art inspection systems and will improve the way gas utilities maintain and manage their systems. Two prototypes, Explorer-I and -II (X-I and X-II), were developed and field-tested over a 3-year period. X-I is capable of visual inspection only and was field-tested in 2004 and 2005. The next-generation X-II, capable of visual and NDE inspection [remote field eddy current (RFEC) and magnetic flux leakage (MFL)] was developed thereafter and had field trials in 2006 and late 2007. It was successfully deployed into low-pressure (<125 psig) and high-pressure (>500 psig) distribution and transmission natural gas mains, with multi-1,000-ft inspection runs under live conditions from a single excavation. This paper will describe the overall engineering design and functionality of the Explorer™ family of robots, as well as the results of the field trials for both platforms. It will highlight the importance of the various design and safety features of the in-pipe crawler and showcase the value of data types and position-tagged visual/NDE data collected in working pipelines under live flow conditions.

1. INTRODUCTION

U.S. gas companies spend more than $300 million annually detecting and repairing gas leaks in urban and suburban settings. The current approach is one of above-ground leak detection and pinpointing (DoT, 1997; Staff Report, 2000), followed by excavation, repair, and restoration (Figure 1). The major cost incurred is typically that of digging and restoring the excavation site (Ives, 1998). Data collected from the Department of Transportation (DoT) indicate that as many as 800,000 gas main leaks are identified in the United States every year. At an average cost of repair of $1,000 each, the problem approaches the $1 billion mark very quickly.

The challenge thus lies in carrying out preventative (rather than reactive) maintenance, allowing for a more cost-effective infrastructure life-extension program at national gas distribution companies (Ives, 1998). The cost drivers thus dictate that the more inspection and repair activities, whether reactive or preventative, can be made from a single excavation, the more cost savings are possible over time (and distance). The cost savings can be dramatic, given that typically one can expect potential leak sites due to a multitude of factors every 50–500 ft (15–150 m), depending on whether the pipe is cast-iron (CI) or steel. Being able to carry out the inspection under live (pressurized-flow) conditions is extremely valuable with substantial cost savings in urban settings, as it avoids the need to carry out pre- and postrepair dwelling (apartment) inspections for safe operation of old-style manual appliance pilot lights.

The challenges for live inspection are mainly equipment/infrastructure and public safety, while minimizing impact of the installation (access excavation) and being able to inspect as long a continuous run as possible in a given time window. These challenges are thus quite different from those faced by inspection systems (and developers) working in the water and sewer industries. Sewer inspection system companies tend to face different challenges, such as debris and biological contamination, making multiphase sensing (air and underwater) harder, yet their access constraints are far more benign (save for sewer gas), also allowing for the use of tethered systems over shorter

Figure 1. Currently employed leak-search and repair process.

Figure 2. Prior art for in-pipe inspection systems.

ranges (Cremer & Kendrick, 1998). Water-supply inspections are typically carried out under fully immersed conditions and can involve pipes of very large sizes, requiring very specialized systems and deployment setups (hydroelectric plants, feeders, etc.). The only other industrial area similar to the one addressed here revolves around oil/gas transmission pipelines; these currently use so-called pigs as fluid-pumped data collectors (Fisher, 1989), requiring offline data processing.[1]

[1]Other Explorer-like work is currently underway to supplement pigs with real-time inspection systems; see Section 12.

In the area of in-pipe inspection systems, there are many examples of prior-art robotic systems for use in underground piping (transmission-pipeline pigs excluded). Most of them, however, are focused on water and sewer lines and meant for inspection, repair, and rehabilitation (Pearpoint, Beaver, KA-TE, GL, NDT, RedZone, etc.). As such, they are mostly tethered, utilizing cameras and specialized tooling, etc. (see Figure 2); a more complete set of systems, including those listed above, can be gleaned from Pearpoint through RedZone. Many of these systems do, however, provide important insight into the different engineering challenges faced in the areas of locomotion (MRINSPECT) (Roh & Choi, 2005), obstacle-navigation (THES)

Figure 3. Representative tethered gasmain (CISBot and GRISLEE) and untethered autonomous (Kurt I and MAKRO) robots developed to date by industry/academia.

(Hirose, Ohno, Mitsui, & Suyama, 1999), and sensing required for the different environments.

Several of the application-relevant (sensing, teleop/autonomous and gas-pipe deployed) systems are (i) the autonomous Kurt I system from GMD (Germany) used for sewer monitoring (not commercial or hardened) (Ilg, Berns, Cordes, Eberl, & Dillmann, 1997), (ii) the articulated, untethered, and self-locomoting MAKRO system from Inspector Systems used for wastewater mains (Paletta, Rome, & Pinz, 1999), (iii) the (albeit tethered) CI pipe joint-sealing robot (CISBot; ConEd-Enbridge), which is deployed through a bolt-on fitting and injects anaerobic sealant into the leaking jute-stuffed joint, and (iv) GRISLEE [Gas Technology Institute (GTI); Schempf, 2004; Schempf, Mutschler, Crowley, Goltsberg, & Chemel, 2003; Schempf, Mutschler, Goltsberg, & Chemel, 2001; Carnegie Mellon University (CMU); Maurer Technology, Inc. (MTI); Porter & Pittard, 1999], a coiled-tubing tether deployed inspection, marking, and in situ spot-repair system (Schempf, Mutschler, Crowley, Gavaert, Skoptsov, et al., 2003; Schempf, Mutschler, Crowley, Goltsberg, & Chemel, 2003). These systems are shown in Figure 3.[2]

Explorer™ represents a promising solution to address the above-stated situation gas distribution companies are facing. Explorer™ is a novel real-time and long-term inspection tool (Schempf, Mutschler, Crowley, Gavaert, Skoptsov, et al., 2005) that allows for rapid and preplanned inspections and repairs wherever needed, allowing national utilities to better manage and allocate their operating and repair budgets, thereby reducing costly emergency repairs. The rest of this paper will describe the system and the testing it has undergone.

[2]A DoE report also offers more insight into pipeline robot systems and their features and comparisons (Schempf, 2004; Schempf et al., 2004).

2. BACKGROUND

To explore the potential of cost-saving robotic inline inspection tools, CMU's Robotics Institute (RI) was chartered to develop an advanced remote and robotic inspection system, capable of multimile, long-duration travel inside live gas mains for in situ assessment and pipe-network cataloging.

The ultimate goal was to develop a generic platform capable of deploying a variety of interchangeable sensor modules and to perform self-powered, wireless-controlled inspections of gas mains at up to transmission-line pressures (<750 psig). The principle of operation was based on performing the inspection without affecting the operation of the network, meaning without pressure/flow reduction or shutoffs. Such a scenario implied the following steps:

- launch the system in a no-blow condition into a live gas main using original equipment manufacturer (OEM) fittings with a custom launcher
- traverse a set distance of pipe while performing nondestructive evaluation (NDE) and visual cataloging measurements
- recover the system by self-extrication of the robot from the main into the launcher under no-blow conditions

The system was to carry out the above steps under self-powered and wireless teleoperation control from the surface utilizing an in-pipe antenna and a surface control system with unidirectional live streaming video and bidirectional status and command-and-control (C&C) data streams.

3. EXPLORER SYSTEM: DEVELOPMENT APPROACH

The Explorer™ system development was carried out in a two-phase program. Initially only the visual-inspection baseline platform was developed, without requiring it to carry NDE sensors and without the need for complete modularity and field serviceability and limited to low-pressure applications (DoE, 2004; Schempf & Vradis, 2004). Owing to the risk and complexity of the envisioned application, the choice was made to first resolve the harder technical problems related to (i) compact integration, (ii) articulation, (iii) wireless control, (iv) self-powered missions, (v) safety considerations, and (vi) the numerous challenges in the mechanical, electrical, and software development areas. This section describes the design evolution for the complete system.

4. PERFORMANCE AND SYSTEM DEFINITION

4.1. Performance Requirements

Utilities required a real-time remotely controllable, modular visual, and NDE-data inspection robot system for the in situ visual inspection and NDE imaging of live 6- and 8-in.-diameter distribution gas mains. It had to be capable

Table I. Ultimate performance requirements for the Explorer system.

Performance requirements
Real-time in-pipe data collection and inspection system
Operation without the use of a tether to reach ±2,500 ft from excavation
Collection of visual and NDE data (varied types)
Inspection capable for 6- and 8-in. diameter pipes in one deployment
Pressurized pipes in the range of in.-H_2O to 750 psig
Operation under low-to-high flow conditions with minimal pressure drop across system
Capable of traversing straight, angled, and vertical (both ways) pipe sections
Able to navigate through various obstacles: short/long 45/90-deg elbows, Ys, Ts
Capable of handling/traversing pipes up to half filled with mud and water
Able to handle pipe- and joint-types for CI and flange-bolted/welded steel
Safe operation in explosive methane/air mixtures
Launch/recovery in vertical and/or angled configurations into a live (pressurized-flow) pipe
Operate on daily shifts of no less than 8 h
Modular design to facilitate module upgrade, sensor exchange, and field maintenance
Maximize traveled distance from single (bidirectional) excavation
Minimize SWaP (Size, Weight, and Power)
Achieve minimum inspection speed of 4 in./s
Minimize down-/recharge time; charging preferrably external due to safety
Provide real-time user interface for data display and robot operation

of locomoting through straight pipe segments and sharp bends, elbows, wyes (Ys), and tees (Ts), including angled and vertical sections. The system had to be designed to operate safely in explosive hydrocarbon environments (methane) and capable of negotiating wet and partially filled (water, mud, etc.) pipes.

Pipe sizes in the distribution network of interest were primarily in the 6- to 8-in.-diameter range, and the system had to transition between them seamlessly. Pressures could range from inches-of-water-column all the way to 750 psig. Launch and recovery were to be performed under live (pressurized-flow) conditions to avoid the complications and cost of a shutdown or bypass. Data were to be collected and time-/position-stamped in terms of both absolute and relative (pipe-/joint-segment based) position. The complete ultimate performance requirements are listed in Table I.

4.2. System Specifications

The system specifications that were generated for the system(s) to be developed can best be broken down into the key categories as depicted in Table II.

4.3. Design Evolution

A programmatic decision was made to achieve the ultimate performance and resulting system specifications using a staged dual-prototype development path. To properly describe the system design variations for the Explorer robot platforms, this paper will focus on the overall final system configuration and provide engineering detail to differentiate between the two incarnations (X-I and X-II) that were developed, when needed. As an overview, Table III details the variations in system specifications and shows how the two variants of Explorer differ in terms of not only their development timeline but also their capabilities and application domain.

The main differences between the two platform systems X-I and X-II is primarily limited to the areas in Table III. Hence in this paper, we will highlight those as they arise and consider all other topics and subsystems identical for both platforms.

4.4. Concept Development and Selection

The concept development and selection process that arrived at the final design of the Explorer robot trains was based on a review of the state of the art at the time (see Hirose et al., 1999; Schempf et al., 2001; Schempf, Mutschler, Crowley, Goltsberg, & Chemel, 2004; Roh & Choi, 2005). Typically design choices are not always related properly or completely in publications, and it is for this reason that we refer the reader to Table IV, where we have documented the decision areas and the rationale used to arrive at the final design. Besides the more obvious choice of a segmented body with module shape and sizes dictated by obstacle navigation, pressure drops, and packaging maximization, the joint configuration (pitch/roll) and placement was driven by practical constraints. Because packaging of drive elements and moving-part simplicity are critical to the utility and ruggedness of fieldable systems, we configured the train with roll joints at each distal drive joint, with all remaining joints remaining as pitch joints in a single plane—namely the plane described by the obstacle or launcher with the installed pipe network. The three-armed design of the drive and support modules was deemed the most compact and efficient to generate the needed traction yet allow maximal body diameter (for packaging internal components), while still being capable of navigating the required obstacles. The choice for commercial radio frequency (RF) components with customized protocols and antenna hardware was driven by pricing and availability, whereas battery selection was driven by

Table II. Overall Explorer system specifications: Categories and numerical descriptors.

Category	Specifications
Length	5–9 ft; adjustable configurations
Diameter	<4 in.; minimizes pressure drop to <1% of line pressure
Weight	35–85 lb; depends on module-train length
Pressure rating	Tested to 1,000 psig
Configuration	Segmented and two-DOF articulated joints; braced traction drive with module centration
Modularity	Multimodule reconfigurability/swapability
Productivity	8,000+ linear ft per 8 h-day (>4 in./s)
Communications	Wireless point-to-point network ISM band with custom protocol and antennae
Power	Onboard (varied chemistry) chemical cells (batteries)
Drive	Triad traction drive
Odometry	Triad encoded wheel followers
Sensing	Dual-ended cameras with fish-eye lens; RFEC sensor; prototype MFL sensor
Electronics	Distributed master/slave architecture; localized high-bandwidth, 8-bit motion control; redundant 32-bit SBC for planning/supervision/comms; high-speed mulidrop CAN bus onboard
Control	Localized PWM position/velocity control with safeguards; high-level position-indexed configuration posture planner
Software	Customized RT 8-bit OS for each module; PCB controller; LINUX-based 32-bit OS with wireless and serial drivers; offboard customized JAVA-based GUI; customized wireless comms protocol
Sealing	Both pressurized and vented enclosures; sealed and coated connectors and PCBs
Safety	Vented and pressurized inert-gas launch/recovery; bidirectional check valve; sealed battery compartment
Operations and logistics	Vertical and angled pressurized launcher; pipe-internal hot-tap antenna with adjustment; in-launcher power recharge
User interface	Real-time video window with front/rear views; supervisory configuration/script planner interface; synthetic CAD display of robot configuration; individual motion override capability for each module (drive, deploy, posture, etc.)

time/cost to implement (NimH for X-I; LiP for X-II). The architecture of a distributed master/slave electronics and software system was mainly dictated by the need to simplify interconnections and realize the use of a customizable operating system (OS) capable of performing the planner computations and communications, while allowing high-speed multidrop communications to 8-bit microcontrollers in each module over a modular network.

Many more-detailed decisions made at the lower subsystem level should become apparent during the detailed design discussion sections to follow and are thus omitted from Table IV.

Table III. Comparison for Explorer family of robots in terms of application and capability.

Attribute	Explorer-I (X-I)	Explorer-II (X-II)
Development timeline	2004–2005	2006–2008
Sensors	Visual only	Visual and NDE (RFEC/MFL)
Pressures	<100 psig	<750 psig
Pipe types	CI flange-bolted steel	CI flange-bolted steel; butt-welded thick-wall steel
Modular	No	Yes
Reconfigurability	No	Yes; multitrain options
Endurance	Medium	High
Battery chemistry	NimH	LiP
Underground locating	No	Yes; EM coil
Redundancy	No	Yes; CPU and RF
Obstacle navigation	Teleop and scripts	Teleop and semiautonomous
Module combination	Drive and camera combined	Camera and CPU combined
SWaP	Shorter (fixed), lighter	Multilength, heavier

Table IV. Explorer robot train design configuration rationale by attribute and subsystem.

Configuration	Description
Robot architecture	
Segmented	Packaging and passage over obstacles and horizontal/vertical pipe sections
Module	
Shape	Cylindrical; maximizes packing volume and minimizes pressure drop
Length & diameter	Combination of both; maximize diameter and optimize length to allow tight cornering while maximizing internal packaging volume
Joint	
Articulation	Dual-end roll joints; all others are pitch joints only
Range	±75 deg to allow for shape following during turning
Arrangement	All planar pitch joints internal to dual-ended roll joints at distal drive joints; allows for simple planar turns to reduce internal drivetrains and planar simplicity
Drive & support	
Arm-triad	Traction force control via preload; centration of module for obstacle/dirt passage
Drive	End-of-arm dual-wheel drive; reduced complexity and more compactness
Encoding	Passive wheel followers in support modules for odometry
Communications	
Wireless	Untethered; OEM parts to reduce cost; modified to suit pipe environment
Protocol	Custom to take advantage of varying pipe waveguide properties
Antennae	Custom; waveforming and pipe internal
Power	
Chemistry	NimH in X-I; simplicity, current drain, few safety concerns Lithium-polymer (LiP) in X-II: energy content, current capacity
Electronics	
Architecture	Distributed to reduce wiring and serial-module configuration Master–slave to allow high-speed control and configuration planning
Embedded SBC	OS simplicity, wireless support, computational headroom
Bus	CAN for speed and robustness
Software	
OS	Linux for low overhead and configurability and open source
8-bit	Real-time kernel to ease and speed development and upgrades

5. SYSTEM DESIGN

5.1. Overall Configuration

The overall serial and segmented design of the Explorer robot platforms X-I and X-II is depicted in Figure 4, with high-level physical descriptors (SWaP) given in Table V. The main differences, other than the length and weight attributed to the multimodule sensor addition, is the fact that redundancy was added to the computing system. As seen in X-I, both distal end modules integrate the drive

Table V. Overall physical descriptors for the Explorer robot trains.

		X-II	
	X-I	RFEC	M FL
Length (in.)	65	99	89
Weight (lb)	35	64	89
# Modules	7:	11:	15:
(excl. steering)	Drive (2)	Drive (2)	Drive (4)
	Support (2)	Support (3)	Support (3)
	Battery (2)	Battery (2)	Battery (4)
	Electronics (1)	Camera and CPU and EM-sonde (2)	Camera and CPU and EM-sonde (2)
	Sensors (N/A)	Sensors (2)	Sensors (2)
	Steering (6) (2-roll/4-pitch)	Steering (10) (2-roll/8-pitch)	Steering (14) (2-roll/12-pitch)
Sensing	Video (2)	Video (2) + RFEC (2)	Video (2) + MFL (2)

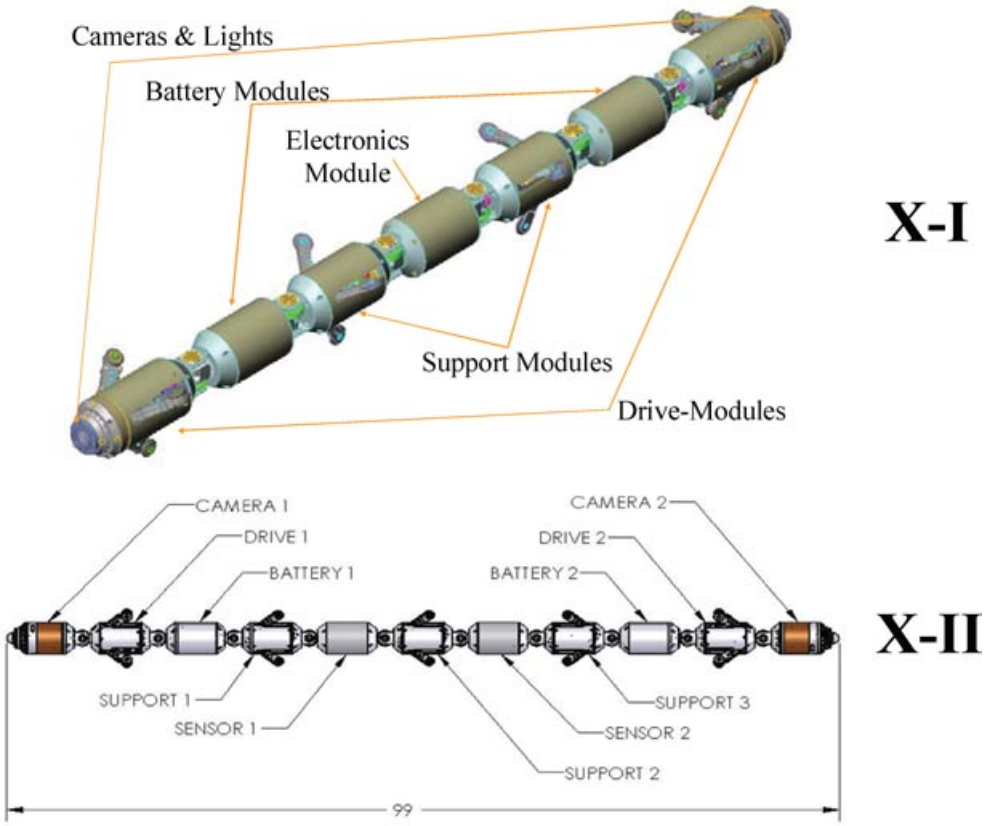

Figure 4. Overall design configuration and configuration for X-I and X-II.

and camera functions into a single module, whereas a central single electronics module is housed in the center module. However, in X-II two separate computing modules were added to each distal camera module, requiring that each drive module become a stand-alone unit.

As can be observed from Figure 4, the design of the robot trains is identical, except for several differences noted in Table V: (i) two additional modules were added in X-II to house the (distributed) NDE sensor modules, (ii) modified and distinct camera modules (video sensor with CPU and EM locating sonde[3]), with (iii) the requisite number of steering joints to interconnect all modules. All modules are modular in the sense that they are field replaceable. The battery chemistry went from nickel-metal-hydride (NimH; X-I) to lithium-polymer (LiP; X-II), requiring the addition of a custom safety circuit and support electronics.

[3]Locating sonde is used to allow for (i) position tagging of noteworthy NDE data in real time and (ii) accurate emergency locating and easier retrieval in emergency situations.

5.2. Reconfigurability due to Modularity

The modularity of Explorer allows for multiple configurations of the robot train in the field, enabling the deployment of different and multiple inspection modalities. This feature is advantageous when an inspection might require a first live video run to make sure the line can be inspected (blockages, etc.), by using a smaller, lighter, and faster-to-deploy/retrieve camera platform, or when sensors that are smaller and require longer range allowing for more battery modules to be deployed. Figure 5 shows such different potential configurations that field personnel have the option to deploy: panels C or B and A, respectively.

The main elements of the design, including the separate modules, as well as the electronics and software for this system, and the support equipment are detailed in the sections to follow.

5.3. System Design: By Subsystem

5.3.1. Locomotion Module

The locomotion system for Explorer is based on a triad configuration of deployable arms, with distally mounted and driven dual-wheel drives. This configuration implements

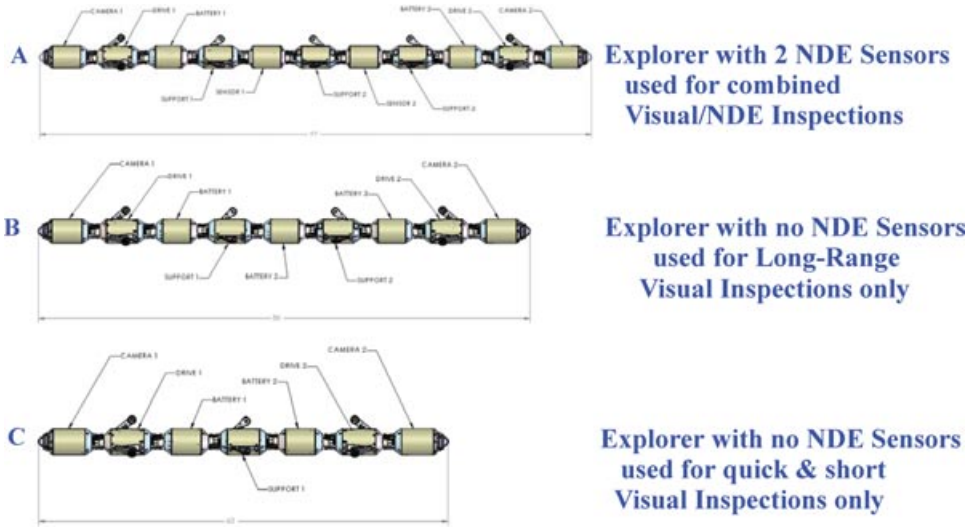

Figure 5. Modularity of X-II affords the use of different configurations in the field.

traction-drive–based propulsion by generating contact forces to create friction to allow pipe-internal driving motions with the module centered in the pipe. The locomotion mode is designed to combine a powered wheel-driven preloadable and adjustable hybrid leg locomotor into a single unit, primarily due to the power efficiency and combined progress travel speed. The architecture of the module is such that the drive module has the ability to collapse its articulated driven arms, allowing it to ride on the bottom of a pipe, but expand to self-center itself in a 6- and 8-in.-ID pipe. The arms are powered by a single motor driving a spur-gear pass, powering a ballscrew to which a nut is attached, which drives the three-bar linkage arrangement to extend/collapse the arms (antirotation feature ensures only linear travel); see Figure 6.

The wheels at the end of each arm are all synchronously driven by a single motor through a planetary gear reduction, with a pass-thru gear train inside each arm, which then powers a dual set of wheels at each arm. The wheel achieves traction due to the compression of the wheel against the inside pipe wall. The unit is sized and designed to allow full vertical ascent and descent inside of pipes, as well as sweeps, bends, Ts, and mitered joints in any orientation.

In the case of X-I, the camera-nose section was added to the drive module to arrive at a robot train with fewer modules. For X-II, the drive module was kept separate from the camera unit. The prototype modules built for X-I and X-II are shown in Figure 7.

5.3.2. Camera Module Section

The camera module is the module that underwent the most drastic redesign between the X-I and X-II iterations of the Explorer robot train. In X-I the camera module was designed as an imaging-only add-on to the drive module, integrating the CMOS imager, fish-eye lens, LED lighting, and protective dome into a truncated cone–shaped submodule. As in all Explorer trains, the "nose cone" of the camera unit was designed as an RF-transparent unit, with embedded antennae on both ends of the robot train. In addition, a set of recharge points was located on the nose cone

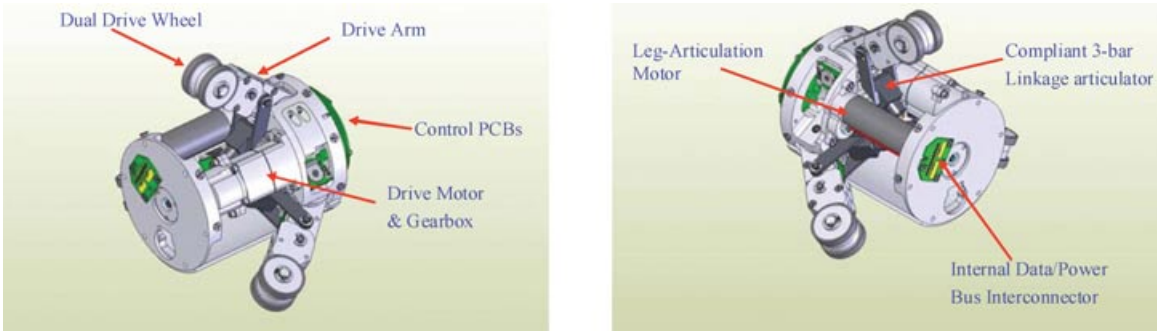

Figure 6. Explorer drive-module design depicting drive-arm triad.

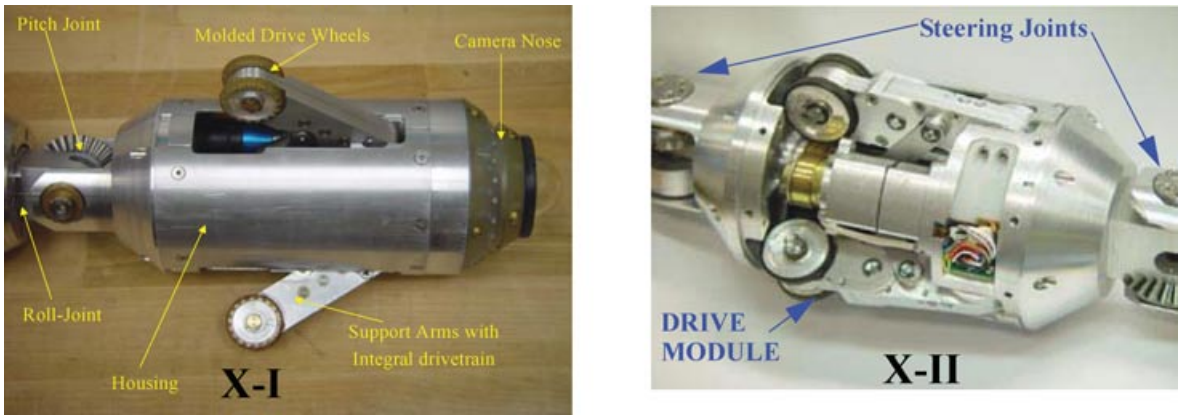

Figure 7. X-I (left) and X-II (right) drive-module design showing integral and removed camera nose.

to allow the robot to be recharged in situ (launcher or external) without requiring any battery-module disassembly. The X-I prototype camera unit is depicted in Figure 8.

The design of the X-II robot train allowed for a separate camera-and-computing module on either end of the train. Compared to the X-I robot train, which had only a single (central) electronics module with a single CPU, X-II provided a redundant and dual computational architecture with a 32-bit processor operating in mirror fashion on either end of the train.

The cutaway view in Figure 9 highlights the location of all the aforementioned elements, including the recharge charger/rectifier circuitry and the electromagnetic (EM) locating sonde and its control circuit. The X-II prototype camera/computer module shows the EM-transparent cylindrical sonde-coil cover.

5.3.3. Steering Joint (Pitch and Roll)

The steering system consists of two types: a single roll joint at each end of each of the most distal drive modules, coupled with a simple pitch joint, and (ii) an actuated one-degree-of-freedom (DOF) pitch joint that allows for the interconnection of all the remaining modules; both of these joint designs are depicted in Figure 10 (the joint design is identical for X-I and X-II).

The steering-joint design is based on two endbells that house a brushless motor-gearbox combination, mounted off axis, driving a bevel gear through a shaft-mounted pinion. The central shaft mounted to the bevel gear has a hollow shaft that penetrates the endbell, allowing wires to be routed through it and hooks up with a bevel pinion gear. Said pinion gear then engages a sector bevel gear that is coaxial with the u-jointed bearing-supported shaft around which the axis rotates. The joint is capable of steering to a ±75-deg angle, limited by hard stops in both directions. Such angular excursions are sufficient to perform the 90-deg turns required of the system. The system contains a "home" limit switch, allowing the system to recenter itself after a power loss. A potentiometer provides absolute position feedback during operation, so as to enable accurate positioning even if power is lost. The motors are brushless commutated stepper motors, with motor-step commands used as open-loop position estimates.

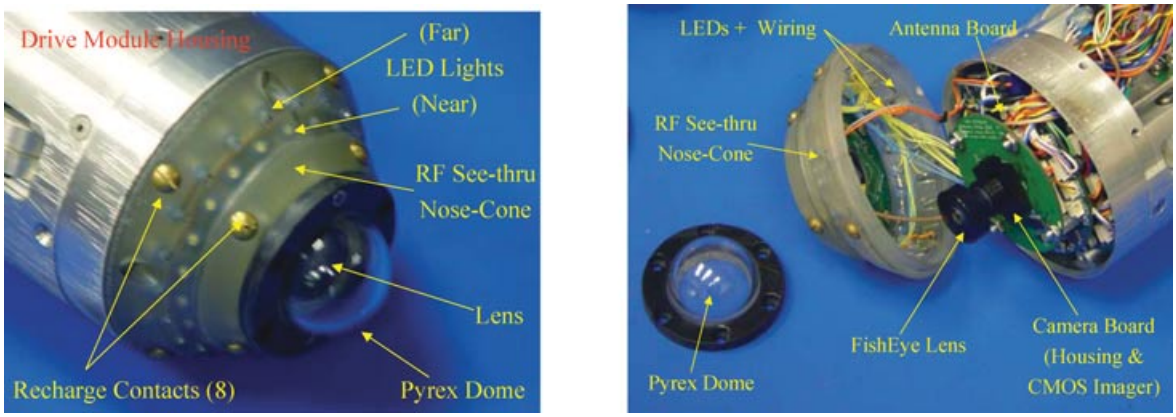

Figure 8. Camera-nose submodule assembly and components of the X-I robot train.

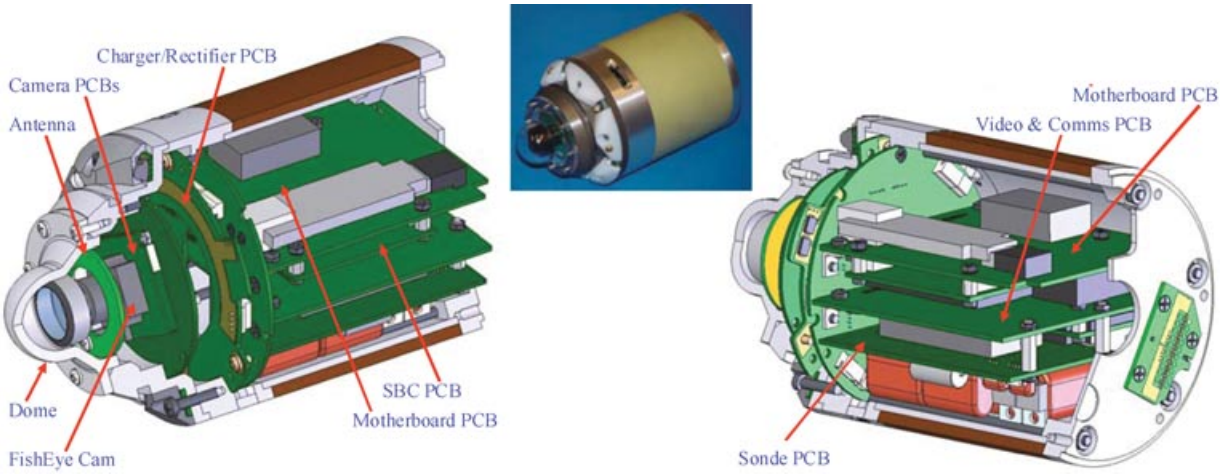

Figure 9. Design of the X-II camera/computer module and the associated X-II prototype unit.

Views of the joint in its straight and angled configurations, as well as the prototype unit (overall and close-up), are shown in Figures 10 and 11, respectively.

5.3.4. Support Module

The support module is necessary to provide centration (alignment with the pipe's centerline) during launching/retrieval as well as climbing and turning to reduce friction and guarantee successful obstacle passage (turns, debris/water, etc.). The design of this module is similar to that of the drive module, in that it employs the same structure and leg-deployment drive design. However it lacks the in-arm, wheel-drive train but rather features an arm with a free-spinning wheel at the end (see Figure 12). The free-spinning arm wheel serves as encoder, using magnets and Hall-effect sensors to provide for a highly redundant position-feedback indicator used by the computer for odometry. On either end of the module are located the steering modules (pitch only) detailed earlier. In addition, each of the support arms is outfitted with a strain-gauge beam arrangement to allow for direct measurement of contact force at the wheel contact point. Such a measurement is important for the arm-deployment controller to optimize traction vs. frictional losses. This additional measured variable was selected rather than extrapolating from motor-current measurements and motor torque-speed curves, which are inaccurate and not overly meaningful for stepper motors, which are used in this module rather than dc motors.

The support-module designs for X-I and X-II are conceptually identical and vary only in minor implementation details. A partially assembled prototype support module with dual-ended steering joints is shown in Figure 13.

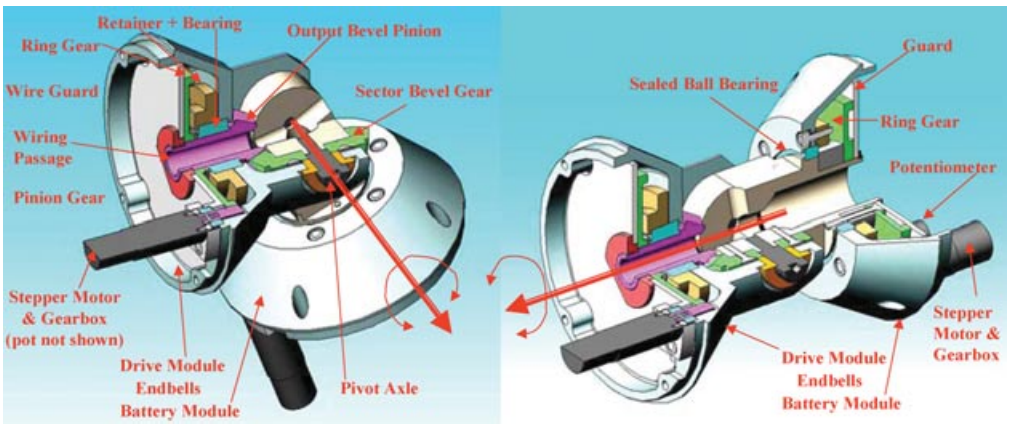

Figure 10. Explorer steering-joint-module design.

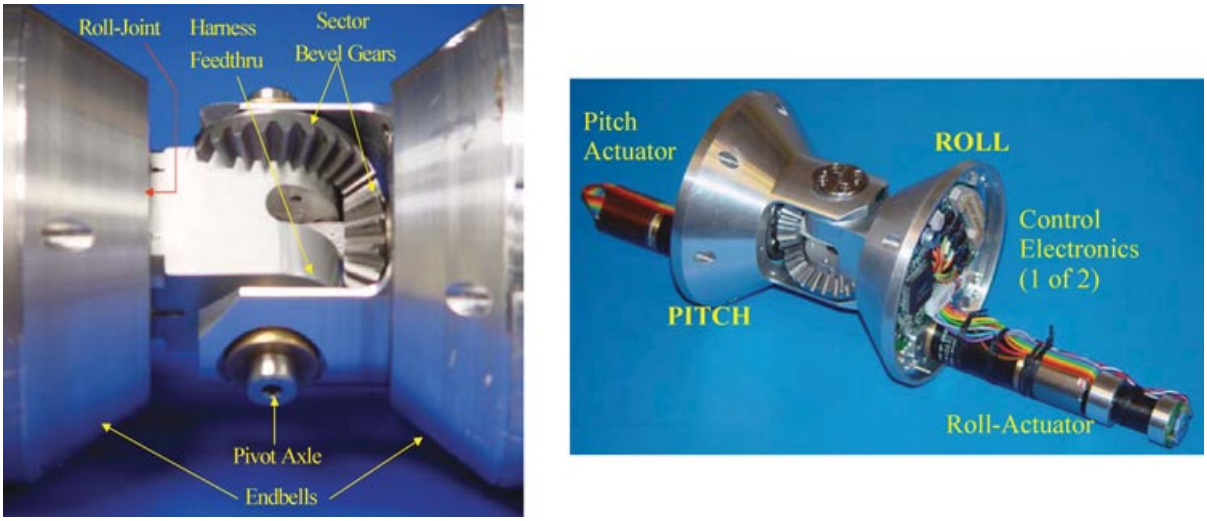

Figure 11. Explorer steering-joint-module design.

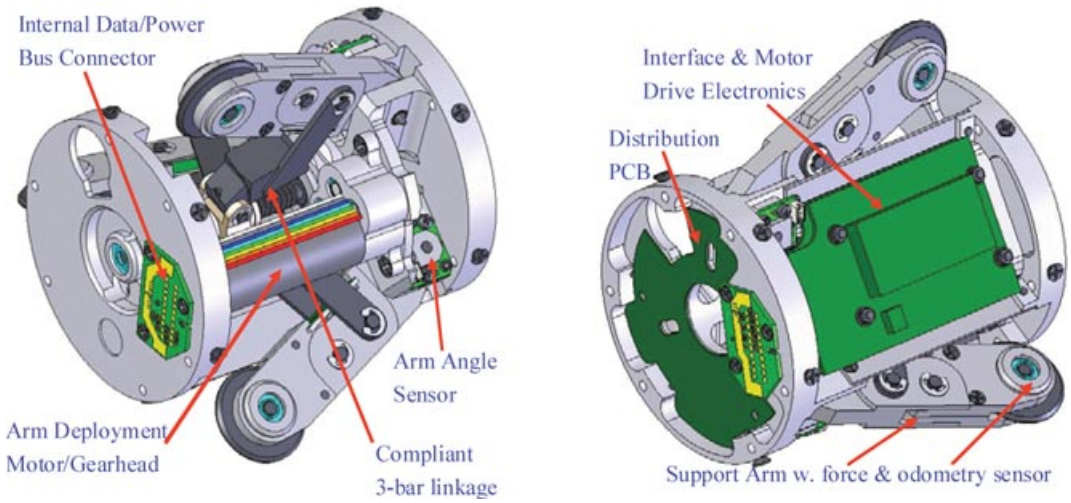

Figure 12. Explorer support-module design and prototype.

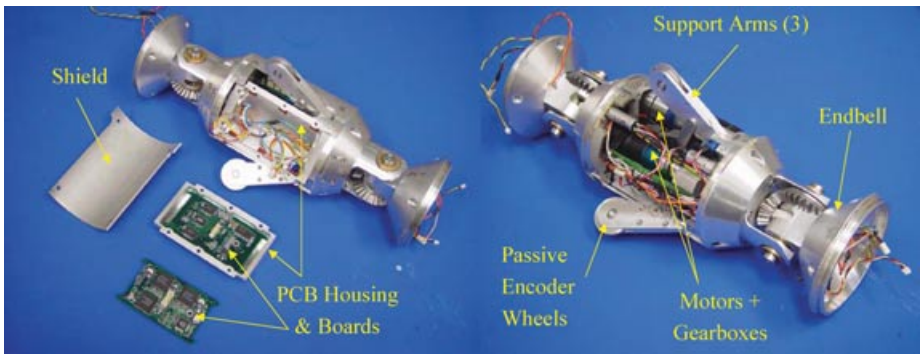

Figure 13. Overall and internal views of the Explorer support module.

5.3.5. Power/Battery Module

The power system for the Explorer family of robots is based on chemical energy storage, namely batteries. The choice of the battery is driven by its use and energy and power requirements. It was obvious that the system had to be reusable, and hence the use of primary (nonrechargeable) cells was not an option. Space was at a premium, and the need for long-duration usage and high-power, short-termed draws necessitated a look at some of the more uncommon cell technologies. Tempered by the fact that the battery pack had to be affordable and buildable by CMU or an OEM within reasonable time and expense, the selection was eventually limited to nickel-metal-hydride (NiMh) and lithium-polymer (LiP) for X-I and X-II, respectively.

An analysis of the necessary power and energy to comply with the single-day mission scenario was developed and agreed to by the utility field personnel. The main assumptions that were made revolved around the following main drivers: weight 35–90 lb (16–41 kg); max. speed 4.5 in. (11.4 cm)/s; frequency or total distance of vertical travel over 2-mile (3.22 km) horizontal travel 1% or 110 ft (33.5 m); equates to (18) 3-ft (∼1 m) rise and drops over 2 miles or a 3-ft rise and drop (bypass) every 590 ft (180 m); deployment duration 8 h; and bus voltage 26–32 V dc.

The resulting power-draw table, including assumed inefficiencies in the drivetrain (50%), the motor (80%), and the amplifier (85%), and accounting for all the hotel-load items (computing, cameras, lights, sensors, communications, etc.), is shown in Table VI.

A comparison of the NimH and LiP chemistries, utilizing OEM cells, yields the results shown in Table VII.

The selection of the battery chemistry for Explorer was based on a combined programmatic and technical decision. X-I uses NimH, as these are cheaper, faster to procure, and safer, require no custom safety circuit, and are easier to integrate overall, despite the increased weight penalty (50% more than LiP) and charge time (8× over LiP). X-II was designated to receive the lithium-polymer cells, allowing for procurement and safety circuit development time and safety validation, so as to achieve a lighter and higher endurance battery pack.

Table VI. Explorer power-draw requirements.

Functional block	Device power (W)	Duty cycle (%)	Avg. power (W)	Energy (W-h)
Drive vert.	61.25	1	0.61	4.90
Drive horiz.	12.25	99	12.13	97.02
Steer	8.00	1	0.08	0.64
Preload	42.00	1	0.42	3.36
Mech. subtotal	123.50		13.24	105.92
CPU	4.00	100	4.00	32.00
Lights	0.24	100	0.24	1.92
RF	1.40	100	1.40	11.20
Support elect.	0.50	100	0.50	4.00
Heat	2.00	100	2.00	16.00
Elect. subtotal	8.14		8.14	65.12
Total	131.64		21.38	171.04

Table VII. Explorer battery chemistry and cell configuration comparison.

	26-V nominal voltage	
	NiMh	Lithium
Dimensions (mm × mm)	17 × 67	17 × 67
Cell voltage (V)	1.2	3.9
# of cells	42	42
Configuration	21s2p	7s6p
Weight (lb)	4.9	3.2
Capacity (A-h)	7.6	7.5
(W-h)	197.6	195
Life (h)	8	8
Charge time (h)	15	2

The design of the power system for Explorer called for a split pack of at least two modules arranged symmetrically along the robot train. The X-I and X-II RFEC-sensor robot trains used said split battery-module system, whereas the X-II MFL-sensor train was able to use a 2 × 2 system utilizing four battery modules evenly distributed along the train (higher energy content due to increased frictional losses and range extension). The generic battery module can best be described as a set of packaged cells, connected to a monitoring (voltage, current, temperature, etc.) and charging circuit board, all housed within the power module in a pressurized enclosure. A cutaway CAD view of the battery module and prototypes for X-I and X-II are shown in Figure 14.

5.3.6. Electronics: Architecture, Module, and SubSystems

The electronics architecture implemented for the Explorer system is based on a distributed architecture. One (X-I) or two (X-II; redundant, mirroring, and computationally load sharing) master–slave embedded 32-bit single-board computers (SBCs) communicate to multiple microprocessors (8-bit ATMELs; typically more than one) in each of the modules over a multidrop serial bus (CAN). Video and digital command data are passed between SBCs in order to allow a combination of video-camera selection and antenna-radiation source and direction selections. In the case of X-II, up to two sensor modules share the power and data bus and also have a dedicated high-speed, intramodule communication bus if needed (USB; 802.3 Ethernet). The resulting architecture of the overall system is depicted in Figure 15, including the offboard, laptop-based user interface and control computer and a separate

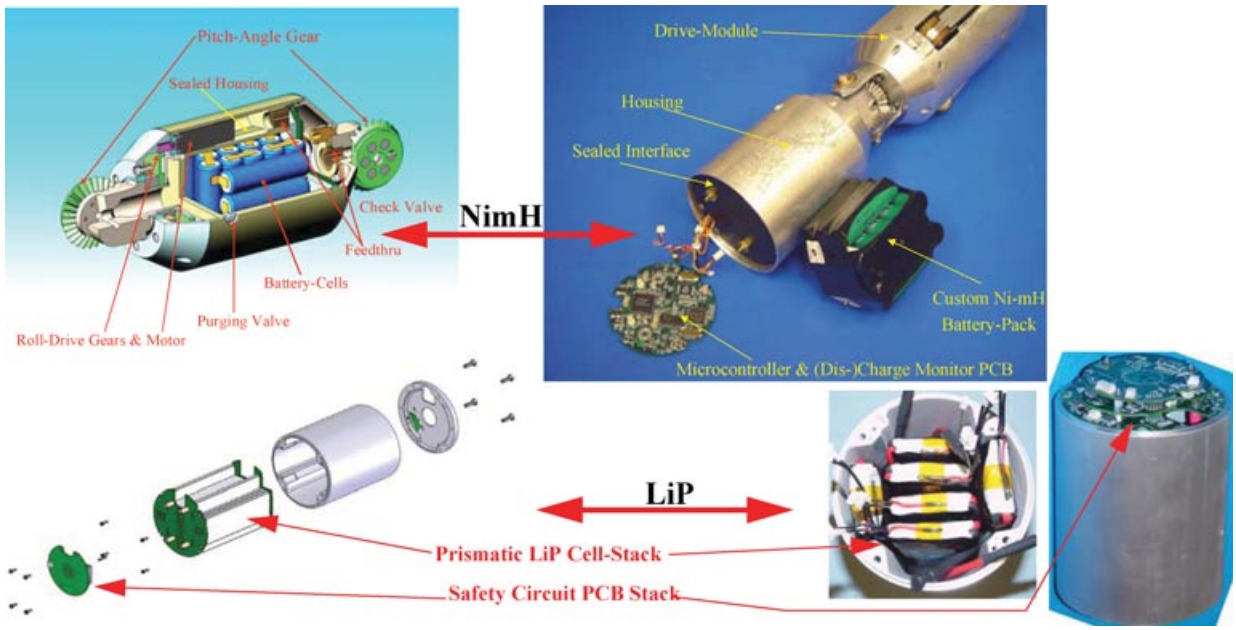

Figure 14. Prototype battery-module design and prototypes for X-I and X-II.

computer for NDE-sensor collection and real-time processing, visualization, and storage.

The resulting implementation in terms of task distribution and data flow over associated bus(es) can best be summarized as shown in Figure 16.

All module-resident microprocessors utilized an 8-bit, ATMEL-based, CAN-compliant processor integrated with custom circuitry on various PCB stacks, communicating over a multidrop serial bus and running a custom-developed, real-time, 8-bit, multitasking kernel. In both incarnations of the Explorer platforms, the central controller (X-I: 1; X-II: 2) was based on a 32-bit processor running on an open-source OS, in our case Linux. The processor board was mounted inside a dedicated cage, including motherboard, I/O PCB, as well as dedicated power-control and CAN-bus interface and control circuitry. A dedicated antenna-switching and custom-developed wireless RF-stage interface PCB was also part of the stack, allowing for complete control over all on- and offboard (wireless inside the pipe, using it as a waveguide) communications. The design implementations were similar for X-I and X-II, except that X-I utilized a custom PCB based on a 32-bit

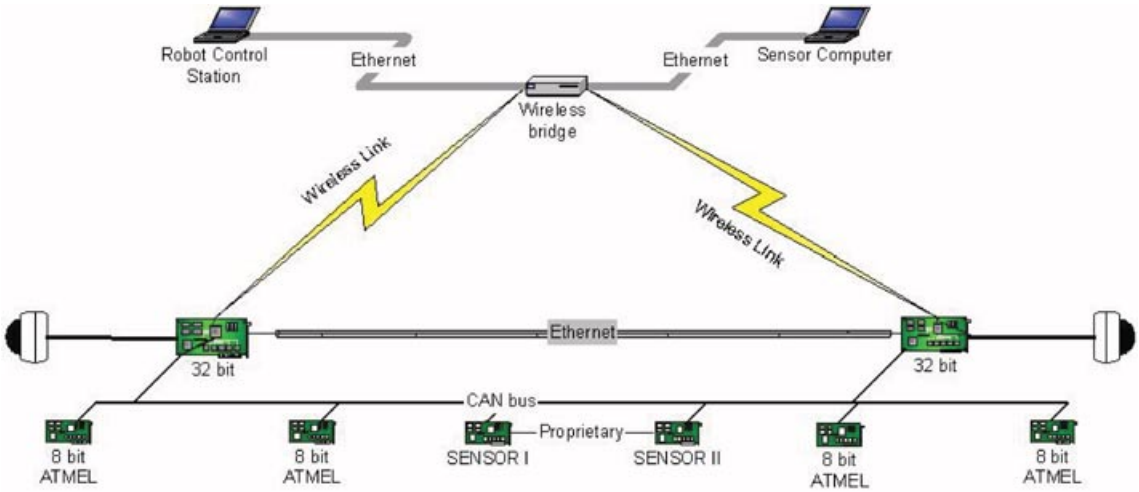

Figure 15. Generic Explorer distributed electronics architecture.

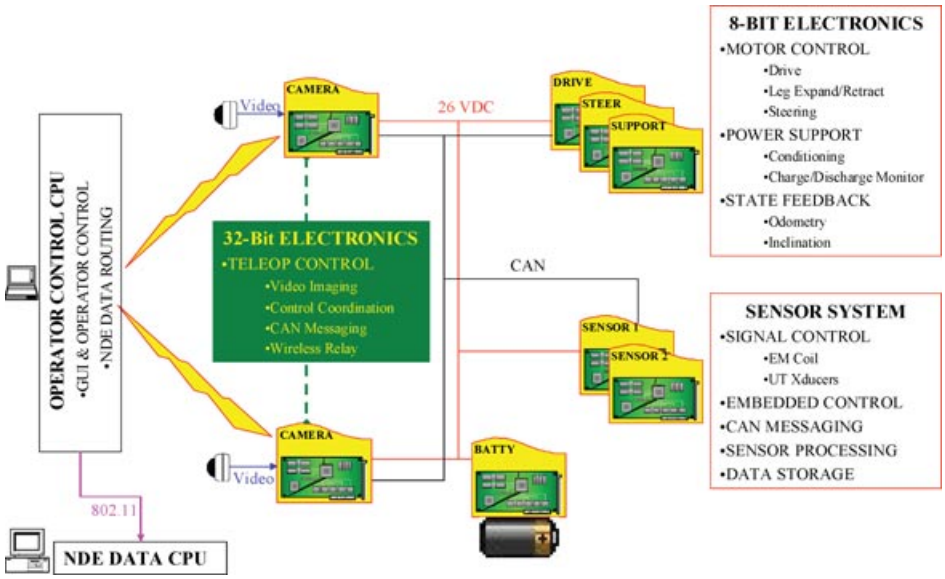

Figure 16. Resulting functional software distribution across Explorer's processor (locations) and interconnecting power (dc) and data (wireless, CAN, 802.15, RS-170) buses of various types.

Hitachi SH4 processor, whereas X-II relied on an OEM SBC based on an ARM processor (a CAD design image of the X-II CPU stack is depicted in Figure 9).

Images depicting the hardware prototypes for the X-I and X-II central 32-bit controller computing stack(s) are shown in Figure 17.

5.3.7. Control: User Interface and Obstacle-Passing Approach

The control of the Explorer line of robots is based on a combination of real-time teleoperation using the high-speed wireless link (video and C&C), as well as scripted semiautonomous obstacle-passing behaviors executed in a (block-wise) supervisory mode.

The portion of the operation carried out in a teleoperated mode consisted primarily of the straight-pipe driving and feature-inspection (visual and NDE) activities. The only level of automation was that of cruise control, in which the operator could set the driving speed (inches per second) of the robot train while watching the monitor and holding an override/joystick controller if needed. The graphical user interface (GUI) used for this portion of the operation

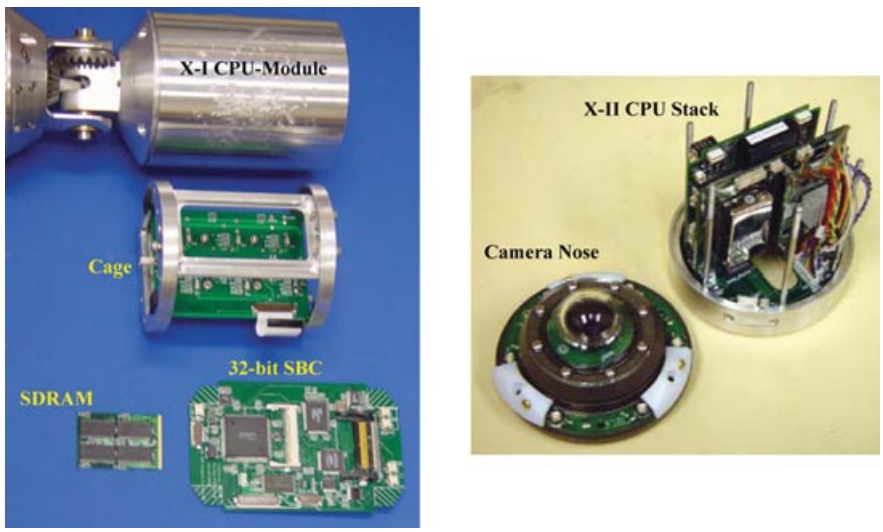

Figure 17. Control and processing electronics unit (left) in the X-I computer (CPU) module and (1 of 2) X-II computer modules (right) resident in the distal camera/computer module.

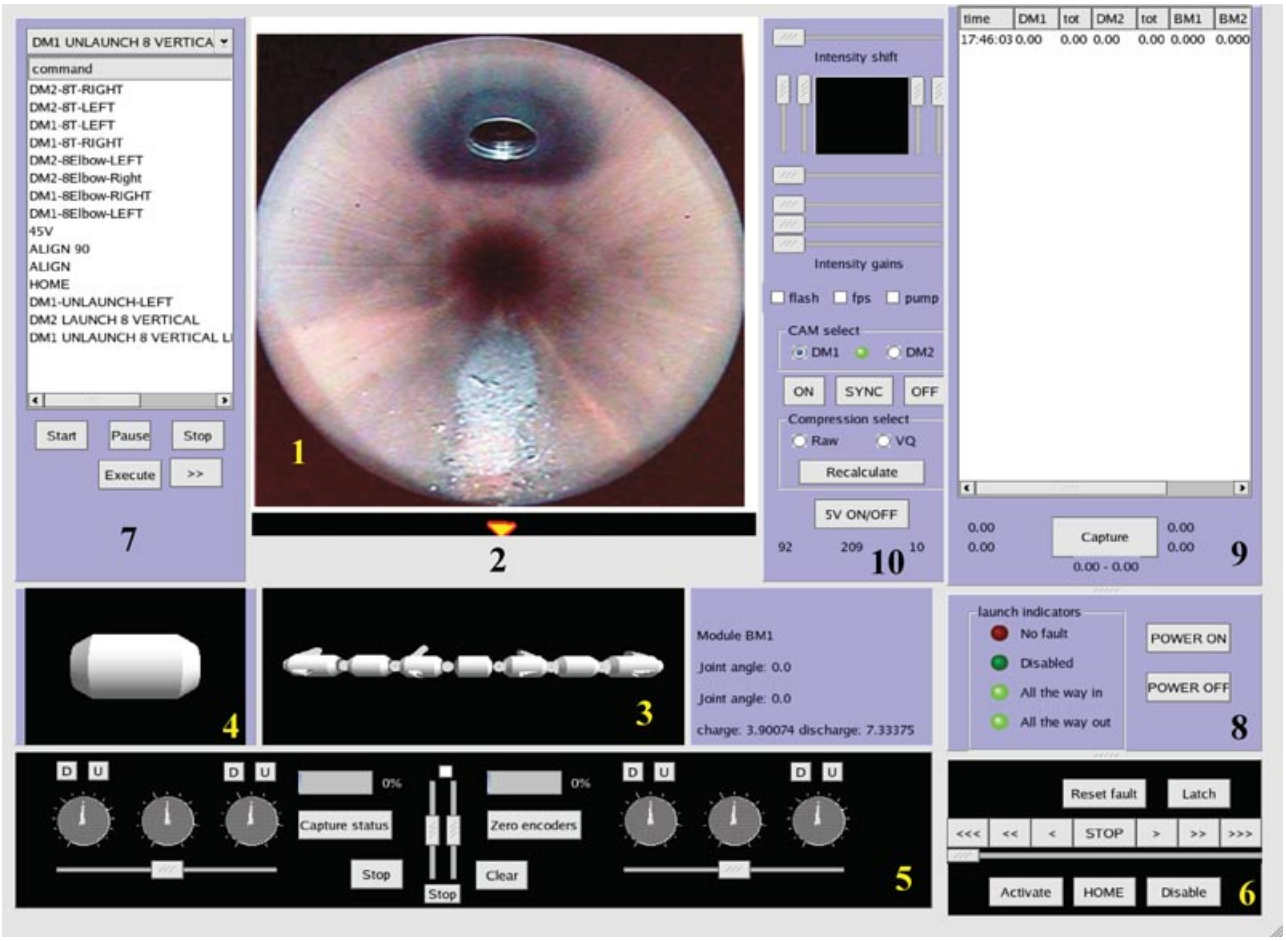

Figure 18. Explorer GUI depicting video window, synthetic CAD image, and inputs.

is shown in Figure 18. The real-time video image (1) shows the front/rear fish-eye view of the camera and depicts the direction of the gravity vector (2).[4] The synthetic display of the robot train (3) allows for viewing of the leg status (open/stowed) and any of the joint angles and drive functions. Clicking on a module allows for a specific module-status display update (4), allowing the operator to then individually control the joint functions (steer, drive, deploy, etc.—if applicable) associated with that module using a set of dials and sliders (5). The semiautonomous configuration planner and executor used for obstacle passing (see next paragraph for more detail) is controlled using VCR-style inputs (6) with a text-based progress update window (7) for feedback. Health-status feedback is presented in both graphic (8) as well as text (9) form on the GUI. Video-image controls (hue, saturation, gain, lighting dim/on/off, camera select) and RF-parameter control (bit rate, frame rate, black and white/color, etc.) are also possible through controls in a separate window (10).

The obstacle navigation is accomplished through a shaped configuration control system. For the major obstacles expected in a pipe network (bends, elbows, Ys, Ts, miters), including vertical/angled launchers (akin to a miter), a precomputed splined path was generated (for each obstacle type) via offline simulation, representing the ideal path that each of the module joints has to follow (see Figure 19). The operator is responsible for locating the front camera image aligned with the edge of the bolted/welded/cut feature, at which point a single button press enables a scripted closed-loop trajectory controller coordinated by the onboard 32-bit SBC. Using odometry from its multiple support module encoders, the system carries out 0.25-in. incremental forward motions with coordinated angular position changes for those joints requiring an

[4]In-pipe robots tend to spiral/corkscrew when driving, making it impossible for the operator to tell up from down.

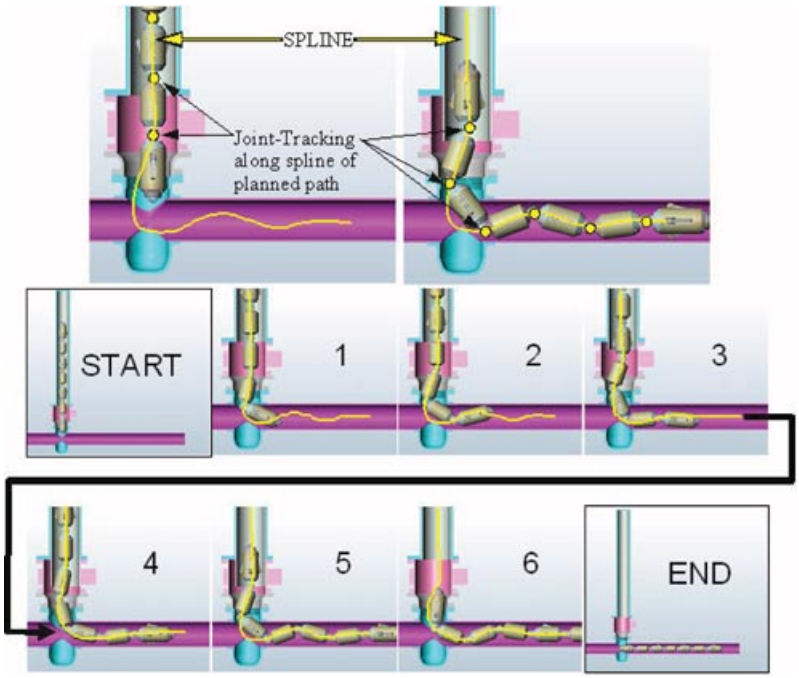

Figure 19. Shaped configuration control time-lapse depiction for Explorer obstacle navigation using a vertical launch sequence (akin to sharp miter bend).

off-axis, zero-angle deflection. This stepwise coordination, combined with collapse/expansion of driving and support arms, "snakes" the robot train through the obstacle, as there is always at least one drive and support module centered and in contact with the pipe to provide traction and encoding. Figure 19 depicts a time-lapse sequence (computer generated) of this scheme for a vertical launch.

5.3.8. NDE Sensing Module(s)

All sensor modules were developed by third parties as part of this program, and hence design details are either proprietary or left to the developers to report as part of their project. The two different NDE sensor modalities integrated onto the X-II include a remote-field eddy current (RFEC) and a magnetic flux-leakage (MFL) sensor. This section contains only an overall description and details as to the prototype assemblies provided by said third party subcontractors.

5.3.8.1. RFEC NDE Sensor

The NDE sensor selected by the sponsors was based on a separate competitive development, demonstration, and testing program funded by the Department of Energy (DoE) and DoT (2006) and resulted in the selection of a RFEC sensing system. The primary sensor design from SouthWest Research Institute (SwRI) was selected to be integrated onto Explorer (X-II). The sensor module itself works on the principle of measuring variations in the remote magnetic field by sensing variations in eddy currents established by an active electromagnet.

The SwRI RFEC sensor achieves this measurement by using a doughnut-shaped electromagnet (excitation coil) housed in one of the two sensor modules to generate the remote field and deploying an array of sensing coils on multiple spring-loaded arms from the second sensor module to close contact with the wall; see Figure 20 for a view of the preprototype RFEC unit used for DoE/DoT evaluation and qualification (DoT, 2006). Dedicated analog and digital processing electronics sample and provide a field-strength measure every 0.1 in. (2.5 mm) circumferentially, based on as many as 12 circumferential measurement points; said measurement points are position tagged based on position data from built-in encoder wheels. The data are not only stored local to the sensor but also compressed (subsampled and reduced) and sent over the onboard CAN data bus to the control computer in one of the robot's nose modules. They are then sent wirelessly to the remote operator station for logging and display on a separate sensor-data visualization computer. An image of the two sensor-module sections (detector and exciter) is shown in Figure 21. Note that the electronics are housed in one of the two modules, including the exciter (electromagnetic coil) and detector. The sensor elements on the detector are arrayed on deployable shoes (akin to an umbrella), which can be deployed or collapsed on command, resulting in open and deployed configurations as shown in cutaway pipe views in Figure 21. More technical detail

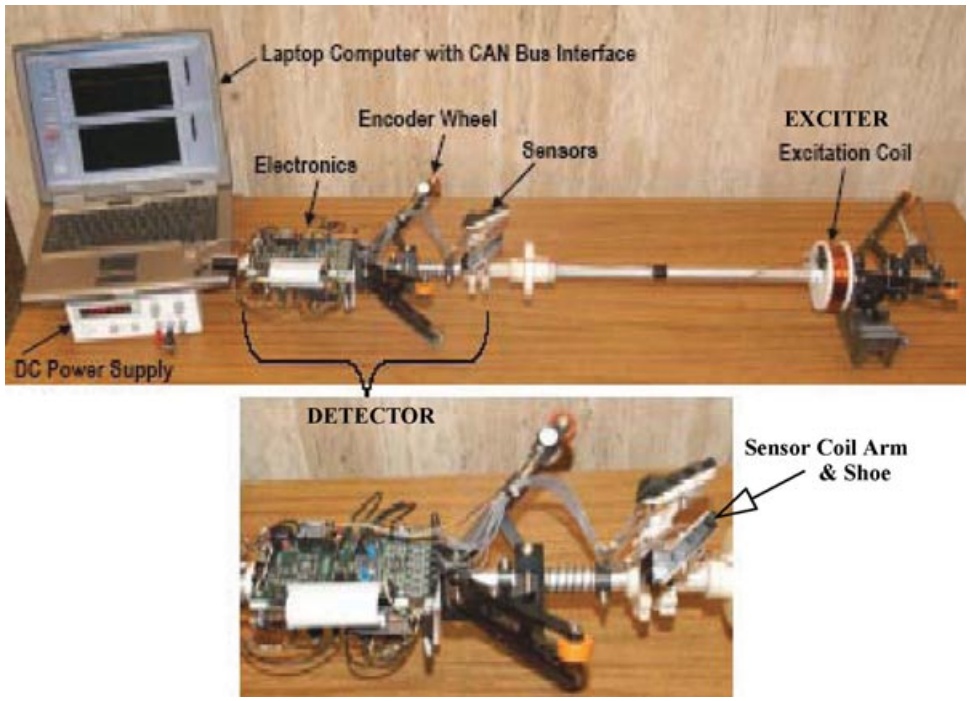

Figure 20. RFEC dual-module preprototype sensor system.

on this third-party sensor from SwRI can be found in key references (Burkhardt, 2007; Burkhardt & Crouch, 2006, 2007; Burkhardt, Parvin, Peterson, Tennis, & Goyen, 2007; Crouch & Burkhardt, 2006; Schempf et al., 2004).

5.3.8.2. MFL Sensor Module

The second NDE sensor selected by the DoE for evaluation was an MFL sensor. Owing to limited funding, no fully functional OEM sensor could be developed. This required that CMU, in coordination with its main subcontractor (Automatika, Inc.; ATK), build and integrate a nonsensored (yet magnetically active) MFL module to allow for traction and locomotion testing. The notion was to collect data for future sensor developers to better target their sensor development to suit the Explorer platform. To support the deployment of the heavier and magnetic-drag-inducing MFL mock-up sensor, additional drive/battery/steering/support modules had to be integrated into an extended-length X-II platform. The extended-length X-II could then be used as a test train, to assess the feasibility and develop guidelines for the future development of a field-deployable MFL sensor module.

The MFL module was designed to allow for both collapsed- and expanded-shoe configurations when integrated onto the robot train, allowing for all data/power/network cabling to be passed through the hollow center. The second sensor module (sensor electronics module) was retained in the train and represents the volume for packaging any support electronics. The suspension and centration springs built into the MFL module are visible in Figure 22, which depicts the sensor in its collapsed/expanded configuration and also integrated onto the extended train platform.

The reduced-function MFL sensor mimics the configuration and magnetic drag effects of a real MFL sensor. Magnetic drag effects are simulated with permanent neodymium–iron magnets mounted in shoes designed to slide along the pipe walls. The MFL sensor has two operational configurations—deployed and retracted. In the retracted state, the shoes are collapsed onto the body of the MFL, whereas in the deployed state, a spring mechanism presses the magnetic shoes against the pipe wall deployed by a set of parallel-linkage arms. The MFL needs to be in the retracted state while not sensing to minimize parasitic drag, as well as allowing for sharp elbow turns. The MFL sensor shoes are deployed prior to the sensing operation, so that the magnetic shoes are pressed against the pipe wall. Figure 22 illustrates the two states in the pipe: to the left, the retracted MFL in the nonsensing (ready for obstacle-passing) state, and on the right, the deployed MFL configuration ready for sensing in the pipe.

5.4. System Design: Operational and Logistics Support

5.4.1. Robot-Train Launch Chamber

In the Explorer family, X-I and X-II used different launcher systems. X-I utilized an angled launcher design for CI

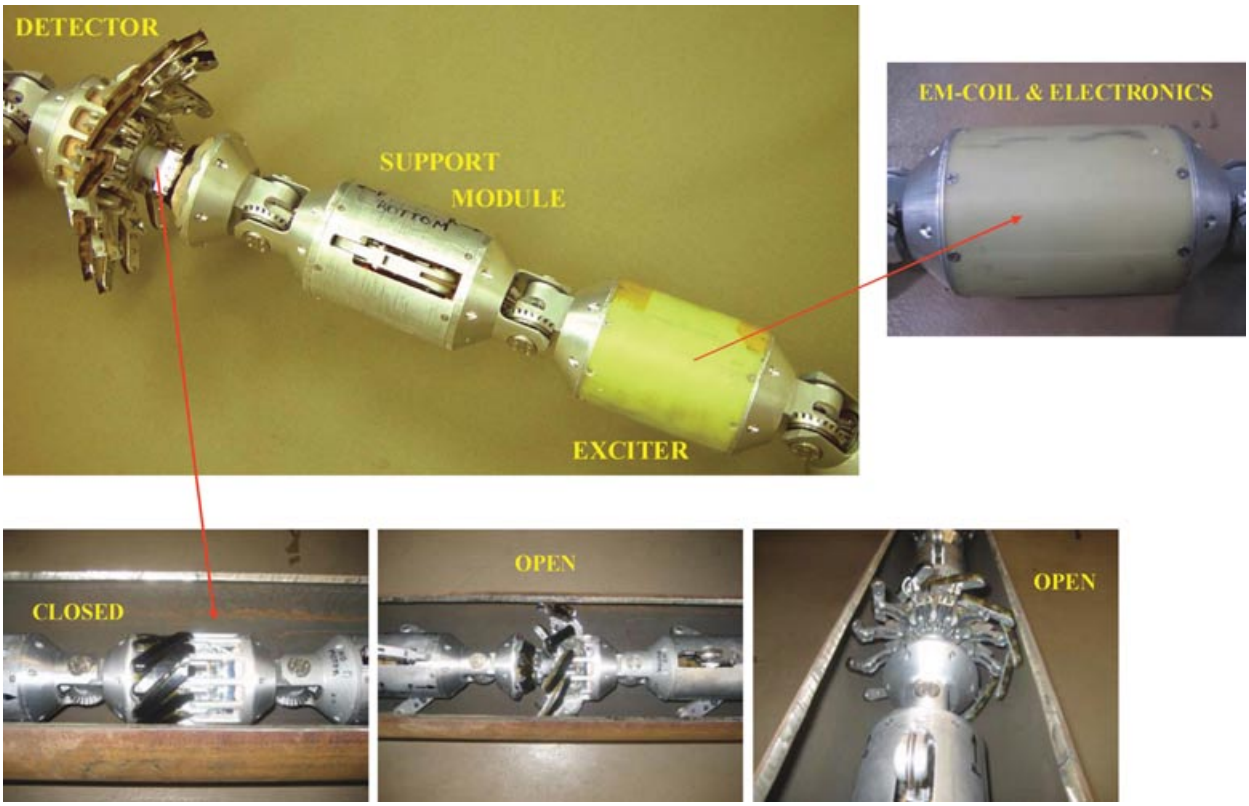

Figure 21. RFEC sensor module elements: exciter and detector in both deployed and closed configurations.

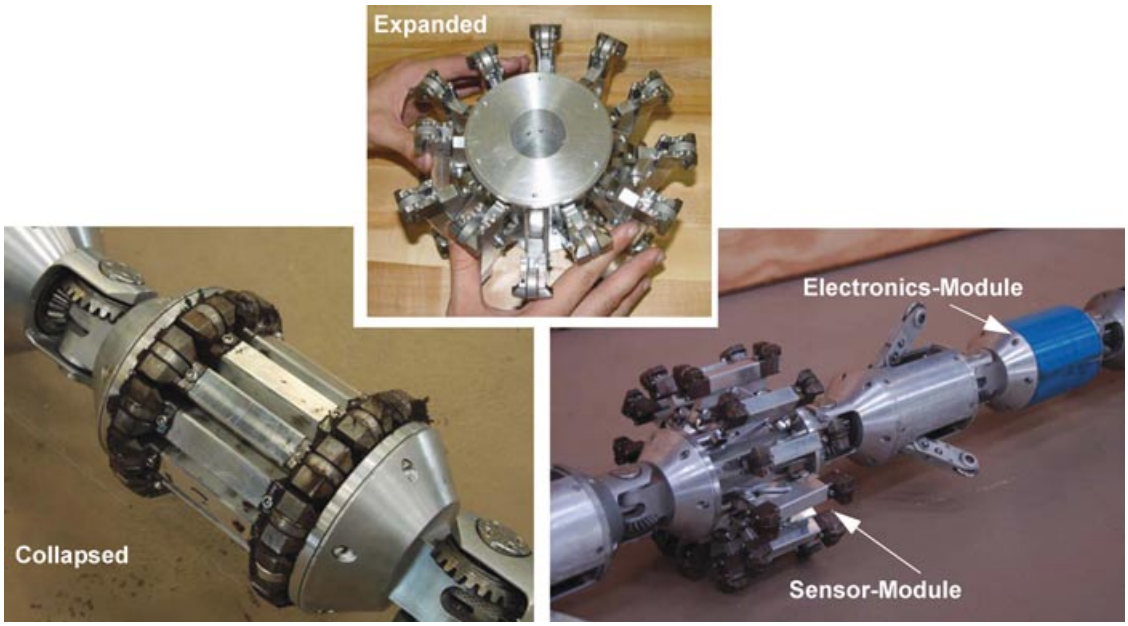

Figure 22. Prototype MFL sensor: collapsed and expanded positions; stand-alone and integrated onto robot train (close-up view), including the sensor electronics module (cylinder).

Figure 23. Low-pressure launcher fitting used for CI mains only.

mains and a vertical launcher design for flanged-steel pipes, driven by the need to keep the excavation costs to a minimum. The X-II system utilized only an angled launcher due to the fact that robot-train lengths and minimal excavation-cost savings did not justify the complexity (size and weight) of a vertical-launcher deployment. Both designs are presented in this section.

Two different systems are used for launching X-I into a live pipe. In the case of low-pressure applications, typically into CI mains, an off-the-shelf relatively inexpensive fitting by IPSCO (flanged bolt on with rubber seals) is used, to which a specially designed launcher tube, carrying the robot, is attached. Different fittings are needed for 6- and 8-in. pipes. The low-pressure clamp-on CI system (allowing for bidirectional launch and recovery) is shown in Figure 23.

In the case of high-pressure applications (in excess of 1–2 psig) for X-I, a specially designed vertical launch chamber was mounted atop an OEM fitting that is welded onto the pipe and post drilled. The reason for a vertical design (rather than angled) was to minimize the size (and thus cost to dig and restore) of the excavation and ease the installation and loads onto the pipe section. The launch tube includes a pressurized internal chamber (see Figure 24) with a vertical power-assist nose clamp that clamps onto the front nose once the camera-module "peeks" into the launcher for recovery (assumes valve has been opened).

The robot is then recovered in a sequence of vertical translations and angular reorientations of the steering modules. The entire launch tube is evacuated of air, purged, and pressurized with inert gas (nitrogen), with all external power electronics for the recovery system housed in an explosion-proof enclosure and driving an explosion-proof motor. The CAD design for the launch tube and the prototype unit are both depicted in Figure 24. In both cases (low- and high-pressure launchers), every effort is made for the excavation to be dug in a "low-cost" location selected by the utility, where custom-installed pipe antennae are used to link the operator console to the robot. During the deployment, the operator controls the robot using a simple forward/reverse joystick interface, while the onboard computers generate all the individual joint-steer and driving commands.

In the case of the X-II platform, launching and recovery had also to be accomplished under live (pressurized flow) conditions, but the launcher was configured as an angled fitting (custom made). It requires that the fitting be welded onto the pipe and then (hole-saw) drilled out with a flanged gate valve providing the isolating seal. The gate valve is installed atop the welded-on fitting flange and the launcher tube mounted to it; see Figure 25.

The indoor test setup for launch/recovery and pipe driving (with elbows and Ts and Ys) depicts the complete pipe installation in Figure 26; the launcher tube and the fitting and pipe sections for final launching/recovery testing as well as field-trial use are also shown in Figure 26.

To load the robot onto the launcher and prior to launching (or after recovery), the robot train needs to be retained in the launch tube. This is achieved through a simple locking endcap (see close-up view on top left of Figure 26). The launch-tube locking endcap houses a manual cam lock to allow the robot to be held in place by the nose cone, as well as containing a passive proprietary antenna rig to allow real-time communications with the robot during launching and recovery.

5.4.2. Pipe-Communications Antenna

To communicate in real time with the in-pipe robot, our partner ATK developed a no-blow weldolet installable antenna (including the proprietary alignment insert and antenna PCB). The antenna is a custom PCB-printed transceiver housed on a rotary bearing to allow for post-installation alignment using a custom tool. A coaxial pressurized feedthru bulkhead connector provides the connection between the antenna and the remote operator console. The complete parts and assemblies are depicted in Figure 27.

The installation of the antenna plug is carried out using a standard TDW weldolet, gate-valve and tapping tools, a modified installation chamber, and updated procedures. Once installed, the antenna itself is inside the pipe void and can be oriented to maximize receive signal strength indicators (RSSIs). An image of the installed antenna in a test pipe is shown in Figure 28.

6. EXPLORER PROTOTYPES

6.1. First-Generation X-I

The first-generation Explorer robot train, dubbed X-I, was the visual-inspection-only platform designed for low-pressure live mains. It was the shortest and lightest platform configuration and was critical to the successful development of X-II, as it provided answers to many

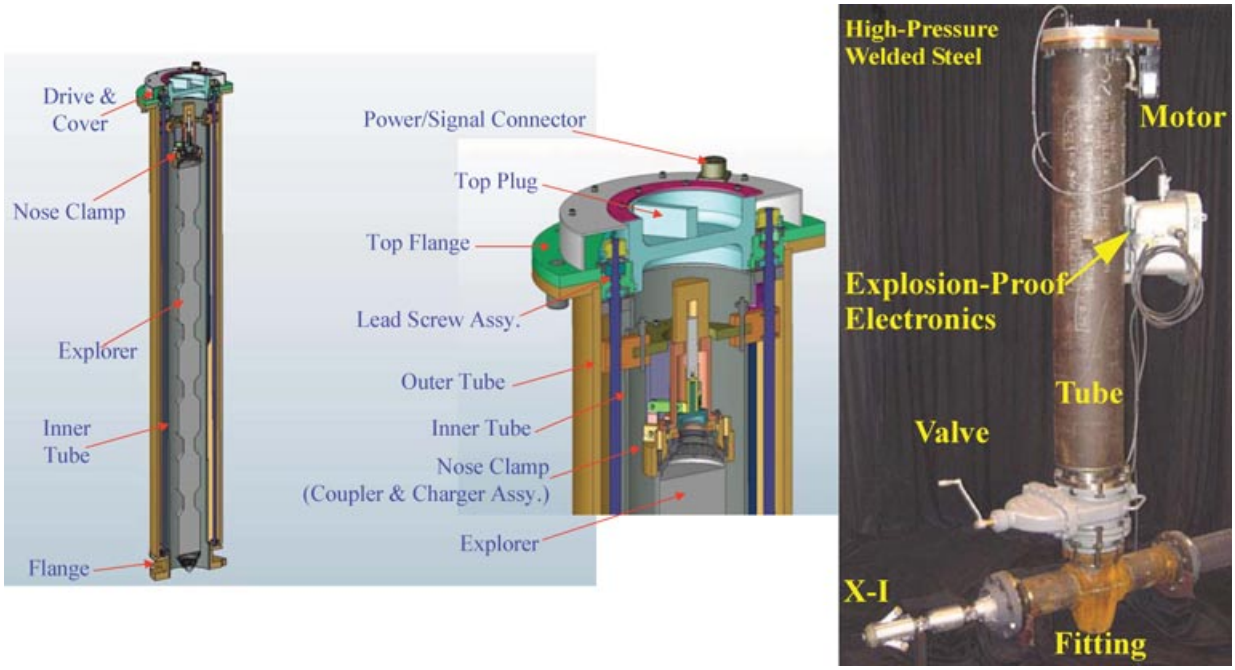

Figure 24. Live-access launching hardware systems: higher pressure steel use only.

technical questions and guidelines for never-before-built subsystems. The prototype platform with all its modules (see labels), applicable pipe sizes, and test pipeline setting is shown in Figure 29. Note that it has *no* NDE sensor as part of its modules but uses solely cameras for visual inspection.

6.2. Second-Generation X-II: Final X-II Prototype Trains—RFEC and MFL Sensing

The X-II (robot-train) platform, in its fully configured state, including all modules (drive, steering, support and battery) as well as the front and rear camera modules, is depicted in Figure 30. Notice that X-II has an RFEC NDE sensing

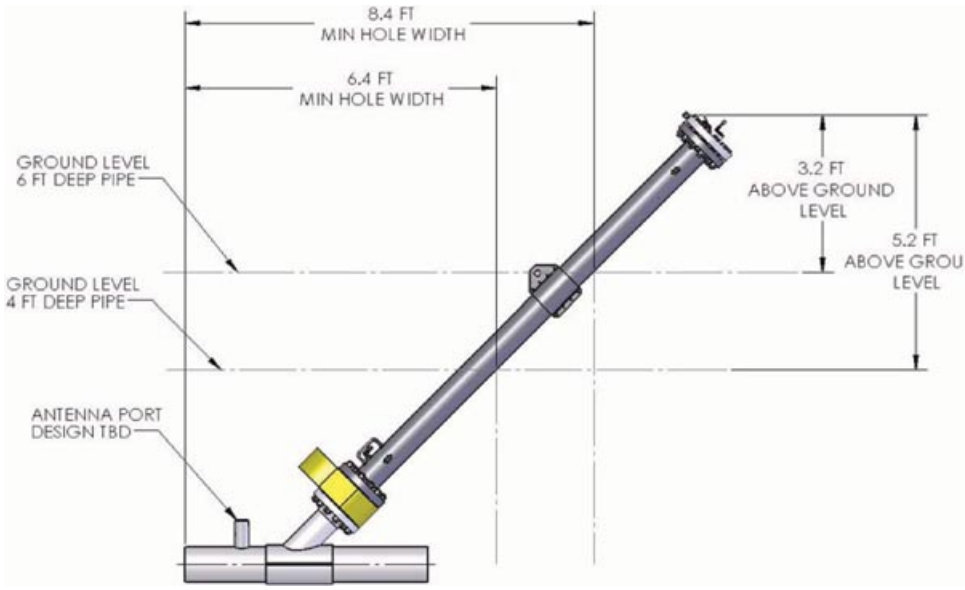

Figure 25. X-II launch-chamber design with fitting on pipe section, gate valve, and launcher tube.

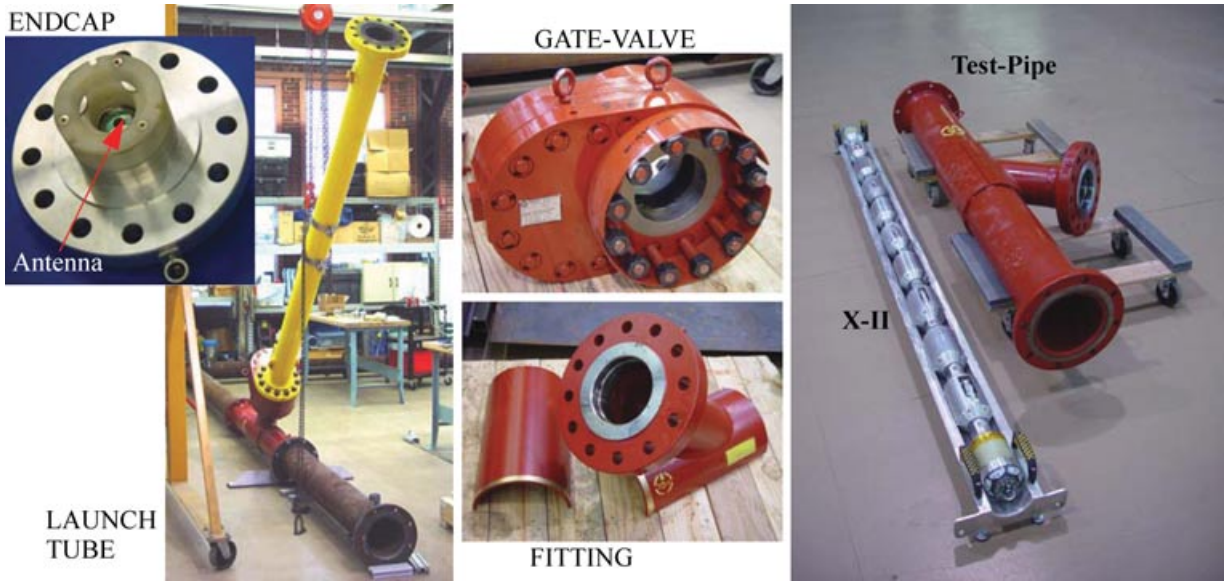

Figure 26. Launcher tube, fitting, valve, and test-section prototypes next to X-II in a launch tray.

module with the exciter (EM coil and electronics) and detector (deployable sensors on spring-loaded shoes) modules in the train.

The X-II platform, including additional drive (two each), battery (two each), support (two each), and steering (four each) modules required for additional power-, traction, and support functions for the MFL NDE sensor (beyond what would be needed to deploy the RFEC sensor), is shown in Figure 31. Note that the overall system is longer (and thus heavier) in order to "support" (traction, range, endurance) the MFL NDE sensors, compared to the RFEC NDE sensor. Said modules were incorporated on both ends of the train (in equal numbers) right after the sensor/camera module. The system continues to retain its symmetry, allowing the use of the generic controller used to run scripts to perform obstacle maneuvering including launching.

7. SYSTEM TESTING

7.1. First-Generation System: Explorer-I

7.1.1. Field Trials

The X-I robot system was fielded into a live 8-in. low-pressure CI main (operated by Consolidated Edison of New York) installed in 1893. An excavation with a one-sided

Figure 27. Antenna prototype as developed by ATK and adapted for use with Explorer.

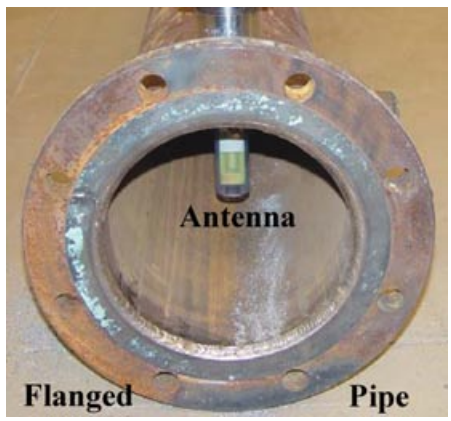

Figure 28. Installed in-pipe communications antenna inside a flange-bolted test-pipe section.

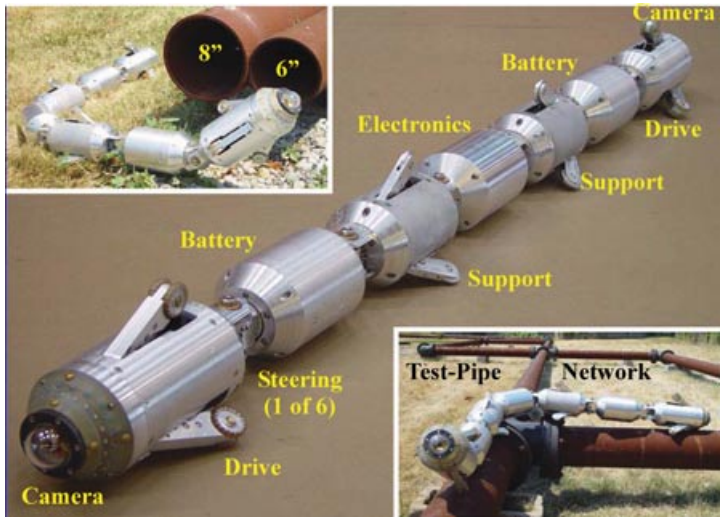

Figure 29. X-I pipe inspection system depicting its modules and pipe-size/-network capability.

IPSCO fitting and a purgeable/pressurizable see-thru launch tube was used in the trials. The robot was launched and recovered multiple times during the multiday test period (see Figure 32).

On average, over a typical 6-h (conservative) deployment period (including launching and retrieval), the system was able to travel more than 3,000 linear feet (∼1 km) and made several T-turns in the main. Wireless range was the limiting factor, reducing the total maximum travel distance on a single battery charge. Features in the pipe such as taps (mapped and unmapped) with associated filings and debris (including beer-bottle caps from the original installation days) were clearly visible (see Figure 32, bottom right). Overall the performance of the system solidly met every criterion it had been designed for—it represented a milestone in both robotics and the gas-utility industry, in that this was the first successful deployment of a fully tetherless and wireless remote-control inspection tool into a live underground gas distribution main.

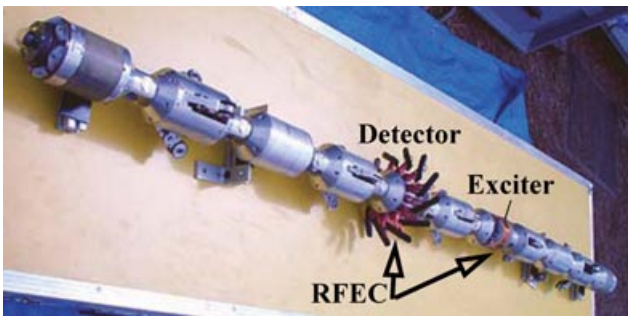

Figure 30. Prototype X-II-RFEC platform depicting drive, battery, support, steering, and RFEC sensor module(s) for visual and NDE inspection.

The next field deployment of X-I was held in a live 8-in. low-pressure main located in the SUNY campus in Brockport, New York, in the service territory of Rochester Gas & Electric, where a 1979-vintage 8-in., 60-psig main was to be inspected (see Figure 33). The main ran westward from the point where the launcher was installed for more than half-a-mile straight, and in the other directions about 75 ft away there were two back-to-back elbows (one 90 and one 70 deg) followed by a long straight segment. The field trial lasted a total of 4 days, during which four launching and four retrieval procedures were performed.

The robot covered a total distance in excess of 6,000 ft (∼2 km). During its travel in the pipe it performed eight successful elbow turns. It traveled more than 0.5 mile (800 m) in one direction from a single hole in one run, returning with ample battery power. A number of mapped and unmapped features (Ts and even an unmapped main connection) were verified. The vertical fitting and launcher worked well, with launching and recovery shown to take 30 min each, including all safety steps. Installation of the launcher and antenna was shown to take 30 and 15 min, respectively.

The operator interface was demonstrated to be user friendly, and a remote display for monitoring and evaluation was also determined to be a viable option. Many system improvements were suggested as part of these initial field trials (Schempf, 2004), such as (a) manual control of the system during launching and retrieval, as well as obstacle handling (still required a good deal of training and finesse despite the precomputed scripts and onboard automation), and (b) improved lighting for midrange (1–3 ft ahead) distances in front of the robot.

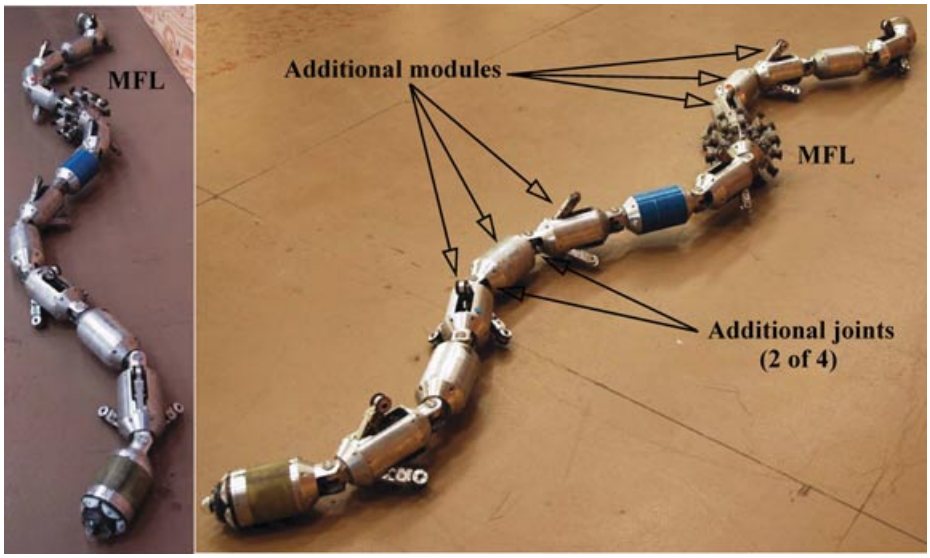

Figure 31. Longer/heavier X-II-MFL platform depicting the additional drive, battery, support, steering, and MFL (functional) sensor module(s) (sensor-electronics module in blue/dark).

7.1.2. X-I Development: Summary and Lessons Learned

X-I demonstrated the ability to provide long-distance inspection of low- and medium-pressure distribution mains in an efficient and safe manner. As part of the multiple deployments and laboratory testing, multiple improvement areas were identified, which were to be implemented in the next generation of Explorer, namely X-II. Improvements lay in the areas of (i) module improvement (use of an OEM 32-bit SBC, ruggedized/hardened drive gearing, dirt shields on arms, larger brushless dc drive motors, arm-on-pipe contact-force feedback, increased-accuracy odometers, better LED lighting, improved obstacle-turn routines) and (ii) logistics support (inclined lower-cost/simplified launcher tube only; no vertical launcher).

7.2. Second-Generation System: Explorer-II

7.2.1. Laboratory Testing

The X-II prototype system was tested for endurance in the indoor and outdoor test loops built at CMU (see Figure 34). A total of 100 ft indoors and ~600 ft outdoors of 6- and 8-in. pipe was available for testing. Only the indoor setup had the launcher attached to it for ease of all-weather testing.

Testing involved launching and recovery of the robot and straight driving, as well as making scripted turns in 90-deg elbows as well as Ts and even Ys—all these elements were CI fittings, attached to flange-welded pipe sections using bolts and gaskets. None of the pipes was seamlessly

Figure 32. Live CI New York field-trial setting in low-pressure gas main and operator interface and visible features (tap and wheel tracks on walls with bottle caps on pipe bottom).

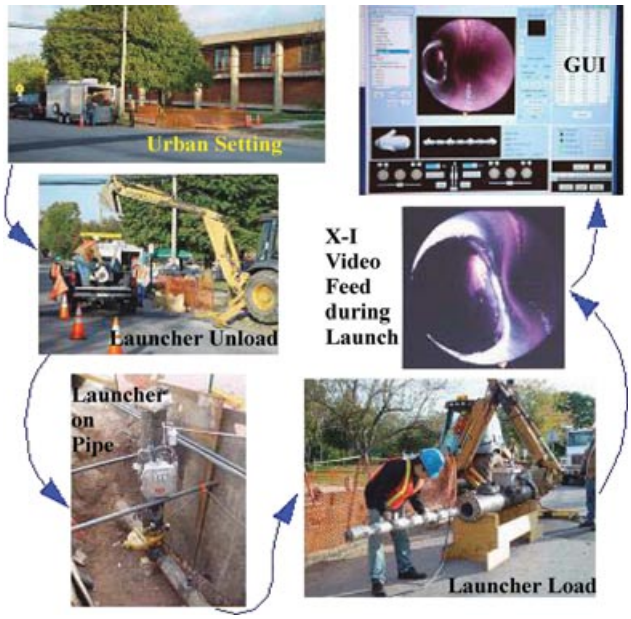

Figure 33. Explorer-I live deployment in a medium (<125 psig)-pressure steel main showing the process of setup, unloading, installation, robot launching, and GUI view during operation (Schempf, Mutschler, Crowley, Gavaert, Skoptsov, et al., 2003).

welded at the joints in order to allow for ease of assembly and reconfiguration.

The testing was carried out over a multimonth period, including several runs with the prototype RFEC sensor; most runs, however, due to lack of continuous availability of the RFEC sensor from SwRI, were carried out with the stand-in mock-up sensor modules (to size and weight). The summary of the test data based on all the runs is depicted in Table VIII.

As is apparent from Table VIII, almost 3,000 m of pipe distance was traveled, with 35 of 41 Ts and elbows having been traversed under computer control, with a smaller number (4 of 8) of Ys and long elbows. A total of 80 launches/recoveries (each counted as a single event) was carried out to refine, validate, and prove the robustness of the device, procedure, and computer-controlled scripts for the robot. Based on all the testing, it was determined that launching and recovery of the 8+-ft-long robot takes on the order of 7–9 min, with any of the elbow/Y/T-turns taking anywhere from 5 to 7 min. This can be considered a very short duration, implying low impact on overall mission duration and robot battery endurance and thus overall range. These data were required by the sponsors prior to the acceptance demonstration (see Section 7.2.2) and prior to proceeding into the field-trial preparation and execution phases of the program.

7.2.2. Pressure Testing: Air and Natural Gas

7.2.2.1. Air Pressure: Testing to Design Pressure

The CMU team used the launcher tube (see Figure 35), with specially fabricated endplates for compressed-gas supply and shut-/bleed-off valves and regulators, to test its X-II system for functional operation in 750-psig compressed air. The goal was to ensure that the entire robot system could operate properly under those pressures without performance degradation. The robot was placed into the launcher, the endplates attached with sealing gaskets, and compressed air fed to the launcher from high-pressure lab bottles, until 750 psig was reached.

The robot's functions (camera, lights, arm deployments, and even short-range driving) were exercised over a period of several hours without any noticeable degradation. The team was thus able to prove proper operation of the complete robot (including the RFEC sensor) in the launcher tube with pressurized air to 750 psig without any component failure being evident. Only a camera lens upgrade was needed (venting/pressure equalization) to achieve tuned focus on the imager to eliminate excessive image defocusing during pressurization. This fault was traced to a sealed volume between the imager and glass cover, which was subsequently vented. No other adverse operational conditions or defects or flaws were detected during the testing procedure. The robot was then

Table VIII. Endurance test data for X-II by distance, obstacle (and type), and launch/retrievals.

	Explorer-II endurance runs						
# of runs	Distance, ft (m)	Sensor?	# 90-deg Ts	# 90-deg elbows	# 45-deg Ys	# 45-deg elbows	# Launches
Multiple	1,600 (488)	No	15	15		—	60
Multiple	300 (92)	Sometimes	10	10	4	—	20
5	600 (183)	Yes	—	—	—	—	—
25	3,000 (915)	Yes	—	—	—	—	—
—	—	No	—	6	—	8	—
26	4,160 (1,268)	Yes	10	10	—	—	—
Total	9,660 (2,946)	—	35	41	4	8	80

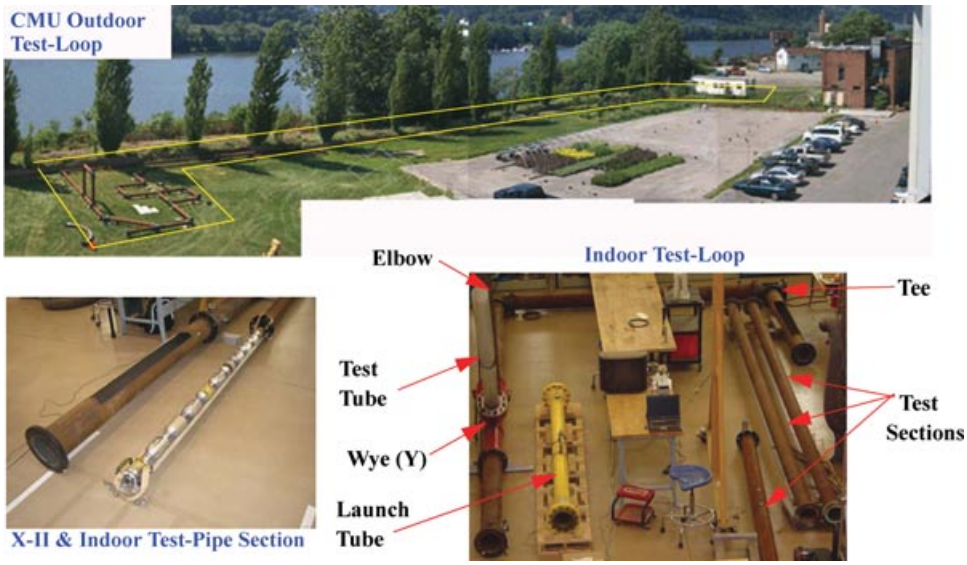

Figure 34. Indoor and outdoor testing facility setups at CMU for X-II endurance testing evaluation.

declared ready for identical pressure testing, but this time in a natural gas (NG) environment.

7.2.2.2. Pressure and Safety Testing in NG

The ultimate safety test for the system, in terms of both the safety design and safety procedures, required the repeat of the pressurized test, but with the use of NG. This test had to be carried out in a specialized facility provided by partnering utilities. The robot and launcher were brought to a NG test station in northwestern Pennsylvania (Henderson), and with the assistance of National Fuels technicians, the system was pressure and safety tested (including all purging and powering procedures) to 502 psig (limitation of the on-site gas station pumping equipment) in NG without any problems and without losing any functionality or degrading the robot's performance. The test proved not only that the system was pressure tolerant, but also that the procedures of purging and evacuation, coupled with the safety design implementations on the platform, were all effective in allowing the system to operate safely in a potentially dangerous environment by exercising the maximum exclusion of the oxidizer, namely oxygen-bearing air.

Figure 35. Launcher tube used for pressure testing to 750 psig for air and NG.

7.2.3. Live Field Trials in NG Main

The ultimate test carried out to conclude the program involved deploying the system inside a live (pressurized flow) gas pipeline in the field. Toward that end, a partnering utility (National Fuels) offered a pipeline near Brookville, Pennsylvania, to deploy and "image" (visual and RFEC-NDE) a live 8-in. steel main operating at around 250 psig. The site is located near the intersection of I-80 and Rte. 28 near Brookville, Pennsylvania. The pipeline carries gas along a sloping highway path with a right-of-way burial access path spanning fields, woods, etc., with the pipeline located at about 6 ft below grade. The pipeline access was excavated, and the site prepared, including various antenna access weldolet points along the multimile-long run available for inspection.

The team spent their 1-week trials performing multiple robot launches and retrievals, installations and removals of the launcher, and multiple antenna installations and removals as part of their testing efforts (see Figure 36).

Figure 36. Typical daily routine inspection activities.

The team also overcame (i) a robot drive failure (with subsequent retrieval and repair for continued operation), (ii) reinstallation of flawed antenna fittings, and (iii) removal of steel coupons from the line prior to being able to complete multiple runs during which the robot collected visual as well as sensory data to provide as a baseline data set for said pipe section to National Fuels, Inc. (NFI), for potential submission to DoT.

A few selected images from the collected field-trial data are shown in Figure 37, including the GUI (robot and sensor), as well as imagery from inside the main showing launcher, clean pipe, taps, and weld seams.

In addition, a preliminary (uncalibrated) data set was collected that clearly shows the correlation between imaged features in the pipe (weld, tap, heat-affected zone; see Figure 38), as well as a set of sensor data verifying that a section of pipe corresponding to the data was seemingly free of flaws and defects.[5]

7.3. X-II Experimental Data Highlights

During the multiday evaluation and field trial, large sets of data were collected and system capability tested and proven (see Table IX), with the X-II robot covering a distance in excess of 0.5 mile in multiple runs. The longest run took it repeatedly more that 1,100 ft away from the launch and antenna point, proving that wireless communications is a viable alternative for live pipe inspection.[6]

A total of six live launches and recoveries were performed, as well as six successful live antenna installation/removal procedures. Owing to unfavorable interactions between the sensor and drive modules with the joints of the pipe, the team was able to collect a total of only ~400 ft of live RFEC data.[7] No pipe-wall measurements related to corrosion degradation were available to the authors yet, leaving us to comment only on visually apparent features detected by the RFEC sensor system. The representative data traces collected and shown in Figure 38 made clear that it was very straightforward to pick out main features in the pipe, such as welds, taps, and even heat-affected (from welding) zones. Identification of these major features in the actual position along the main was possible through correlation of the real-time video feedback from the robot and the observed RFEC data. Additional incremental position correlation is carried out by visually (or via RFEC data-set interpretation) counting the number of full welds and knowing the standard pipe-length sections (utility construction database) and then extrapolating the actual distance from the excavation. If any suspect or major defect is located, the onboard EM sonde can be activated and detected through an above-ground antenna, allowing the placement of an external marker for future follow-up. Note that actual position accuracy of defect location is thus limited to (at worst) odometry error build-up between successive pipe-section weld joints (20–50 ft, depending on pipe diameter), which is very small, even assuming a 1%–5% accumulated error figure for crude unfiltered odometry readings (1–3 ft typically). Because any follow-up on a potential flaw/defect consists of an excavation for external inspection and remediation, and with typical excavations being no less than 3 ft in axial length on a pipe, the achievable accuracies of the Explorer sensing and positioning system are well within desirable operational limits.

Table IX. X-II live-pipe field-trial data.

Parameter	Value
Coverage	
# Live pipe deployments	3
Distance	>3,000 ft
One-way inspection distance	1,200 ft (8-in. welded steel)
Launches/recoveries	
Angled launcher	>8
Obstacles passed (type)	
90-deg elbows	>20 ea.
90-deg Ts	>35 ea.
45-deg Ys	>10 ea.(vertical)

[5]A complete report on the actual data collected was generated by SwRI and delivered to the NGA and DoT as they funded the sensor-provider support separately; see Burkhardt et al. (2007).
[6]Ultimate range is a function of frequency, pipe diameter, and internal pipe-surface conductivity/resistivity.
[7]Said data set is in the hands of SwRI and is part of a separate report from SwRI to the DoT (Burkhardt, 2007), to be published by SwRI and DoT soon.

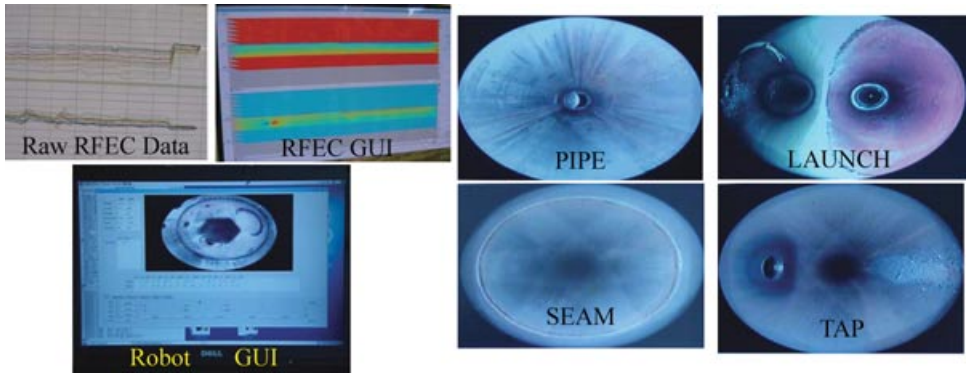

Figure 37. Field-trial data sets collected via X-II in a live high-pressure gas pipeline deployment, depicting the GUI for the robot and RFEC NDE sensor, as well as multiple screen shots of the video from the robot showing various internal pipe features.

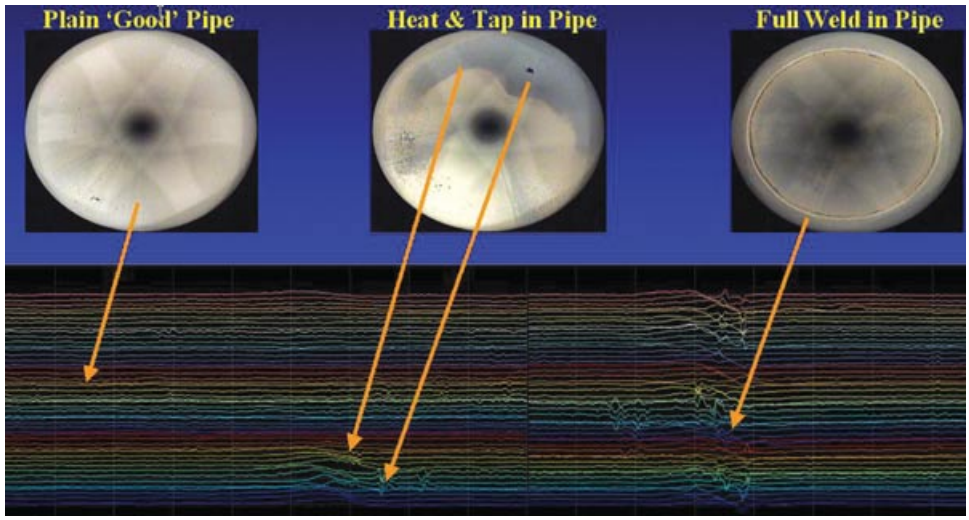

Figure 38. RFEC sensor data of live pipe inspection run showing flawless pipe, taps, and heat zones.

8. SUMMARY

The multiphase, multiyear development and field testing effort for the Explorer family of live visual and NDE inspection platforms for NG distribution and transmission pipelines was successful. It resulted in a novel technical solution to a tough problem and resulted in successful demonstrations and inspections and the transition of the technology and prototype(s) as well as the signing of a license agreement between CMU (developer) and the cofunding gas consortium for the commercialization of the Explorer technology.

A more high-level summary of the technical (engineering and safety), operational, and field-trial results achieved during the technology development program is shown in Table X.

Even though not mentioned explicitly in Table X, it is noteworthy that (i) the overall system design and safety approach were clearly validated in both testing and live explosive-environment laboratory and field tests and (ii) operationally the tools, procedures, and operations hardware were neither foreign nor intimidating to current field crews and trained operators, thereby easing the technology transition and adoption barriers.

9. CONCLUSIONS

The design, development, and field-trial evaluation program for the Explorer family of robots (X-I and X-II) resulted in the development of two field-worthy prototypes for use in (i) strictly visual low-pressure (<120 psig) distribution mains (X-I) and (ii) visual and NDE inspection of live natural distribution and transmission gas mains with pressures up to 750 psig (X-II). To provide a comprehensive summary of the programs' conclusions drawn from the program effort, a list of topical areas and focus elements is provided in Table XI.

Overall, the modular and articulated/segmented design with modular sensor interface proved to be very

Table X. Summary of Explorer program results and achievements in various categories.

System design	
Segmentation	Articulated segemented design proved it could travel trough obstacle-rich pipe networks
Mobility	Steering and drive-joint combination was optimal to access/traverse/navigate networks
Power	Pressurized and vented NimH/Li-P proved to be safe, effective, and customizable
Communications	Wireless links proved their worth; performance a function of pipe type and diameter
Computing	Dual-redundant SBCs and distributed micros were very effective, reprogrammable, and maintainable
Safety approach	
Purging/venting	Nitrogen purging and ventilation were an effective launch/recovery safety feature
Pressurization	Pressurization was an effective option for key subelements; required more procedures
Procedures	Launching/recovery cannot be accomplished without proper proedures for safety reasons
Deployment and operations	
Launching	Vertical and angled; angled was simpler, cheaper, and less power-consuming; fitting costs matter
Antenna comms	Viable inside CI and steel; ranges to multiple 1,000s of feet
UG localization	Odometry drift was substantial (slippage); EM-sonde localization as walk-along worked well
Mapping and display	Simple pen-and-pencil mapping adequate but not ideal (cumbersome, slow, error-prone)
Visual/NDE data collection	Real-time video feedback for teleoperation overlaid well; raw NDE data display proven to work
Logging and visualization	Preferrably GIS overlay onto pipe network with digital image lookup database (ideal)
Field testing	
Coverage	
# live trials	4 to 5
Distance	>10,500 ft
One-way inspection distance	350 ft (4-in. CI); 1,200 ft (8-in. welded steel)
Launches/recoveries	
Vertical launcher	>20 (medium-pressure steel pipe)
Angled launcher	>80 (low-pressure CI—30%; high-pressure steel—70%)
Obstacles passed (type & #)	
90-deg elbows	>50 ea.
90-deg Ts	>75 ea.
45-deg Ys	>25 ea.; both horizontal and vertical

viable and usable in the field. The distributed architecture on a multidrop power/communications bus with a common protocol was very effective and scalable, including the train's configuration/articulation control scripting for obstacle navigation (obstacle-specific and time- and shape-indexed scripting). The third-party sensor integration was smoothed through the use of an interface control document (ICD), allowing for future sensor development and integration with ease. A simple video- and computer-rendered robot configuration GUI was sufficient to allow for sufficient telepresence for remote operations inside a pipe. Field testing validated not only the safe design aspects of the system but also the procedures for effective operations in an explosive environment and inside/outside of NG pipelines. Launching and in-pipe communication fittings and procedures developed for this system proved that they were safe and effective and worth emulating in the future. The RFEC sensor worked well with qualitative data success, with the accuracy (quantitative) of the collected data still to be validated (by SwRI under separate and ongoing DoT funding). The use of an MFL sensor was shown to be feasible, including the development of lessons learned for future sensor developers to consider.

10. RECOMMENDATIONS

The design, laboratory experimentation, and field-trial prototype evaluations for the Explorer program were extremely successful. And as with any R&D and field-validation program, there is a set of recommendations and suggestions that are worth capturing for future refinement and development/commercialization efforts. These have been drawn up in a comprehensive and structured manner and are represented in Table XII.

Overall, this program has provided proof positive that the Explorer-family platform design(s) and prototype(s)

Table XI. Summary of Explorer program conclusions in various categories.

Modular design	System design
Interfaces	Modular interfaces (mechanical and electrical) facilitate maintenance and in-field configuration
Communications (HW/SW)	Common hardware communication bus and software protocols allow for multimodule usage
Implementation	Common nonconnector (PCB contact-pin method) proven to be effective and rugged
Computing	Modular and redundant main CPU module allows for safer operations and technical upgradability
Sensing (type and modularity)	
Overall	Modularity allows for varied sensor usage, upgrade and field exchange/insertion
	Prototypes
Integration	
Overall	Successful integration facilitated with a complete ICD (sensor <–> platform)
Ruggedness	
Overall	Half-dozen live trials deployments with multimile visual and NDE inspection runs
Control software	
Train configuration	Space- and time-indexed configuration controller to shape train to navigate obstacles worked well
Modularity	Multidrop communications bus with local controller architecture supports distributed control
Functionality	
Operator interface	The GUI with live video and CAD shape-rendering provided critical telepresence to operator
	Field testing
Safety testing	
Class I Div. I Certified	Evacuating, purging, and flushing/pressurization design architecture with procedures proven safe
Operations	Safe operation proven to 750 psig without performance degradation
Trials: Low pressure findings	CI launching and travel successful and limited by pipe diameter, standing water, and range
Trials: High pressure findings	Cleaner pipes and better waveguide behavior allows for better NDE data and greater RF range
	Sensing
RFEC module(s)	
Design and data	Unidirectional articulated design was effective; NDE data qualitatively precise; accuracy unknown
MFL module(s)	
Design (only)	Magnetic collapsible sensor mock-up proven viable; processing electronics/software not completed
Robot train integration	
Sensor modularity	Expanded sensor requirements can be accommodated with additional integral robot-train modules
Sensor testing	
Overall	Sensor operation proven; data (raw and processed) quantitative accuracy is not yet established

represent a commercially viable and innovative tool for the inline inspection (ILI) requirements drafted by the DoT for distribution and transmission pipelines that the gas utilities will have to abide by over the coming years. The fact that the technology has been exclusively licensed to a U.S. gas consortium is a testament to the success of this development program, the maturity achieved for the technology incorporated in this system, and proof that government/industry partnerships can be a successful means to drive technology to meet the needs of industry and abide by government-imposed regulations aimed at public safety.

11. FUTURE PLANS

NGA (cosponsoring industrial gas consortium) has licensed not only the CMU-developed Explorer platform technology but also the RFEC sensing system from SwRI, allowing them to sublicense the manufacture and servicing

Table XII. Summary of Explorer program recommendations in various categories.

System design and protoype	
Drivetrain	
Articulation	Design single-piece shaft/gear assemblies in better material at commercial volume/pricing
Wheel-drive	Develop a more reliable metal-to-elastomer bonding process to increase wheel MTBF
Suspension	Increase suspension throw to allow more positive obstacle handling and increased preload forces
Obstacle handling	
Pipe-joint seams	Test new drivetrain, suspension, and anti-drop-in wheel skis to handle wide and deep pipe-seam gaps
Upgradability	
Programming port	Add module-external programming port for speedier upgrades and field-testing modifications
Wireless boot loader	Develop wireless boot loader to increase embedded-software and robot-controller code updates
Operations	
Launcher extension	Increase launcher-tube dimensions for longer future train configurations (longer/multiple sensors)
Sensor development	
MFL sense/control modules	Build an operational MFL system; design areas of interest: flux-shoe, rollers, and articulation
Extended system testing	
Pipe-joint varieties	
Negative/positive seams	Retest with more pipe-seam types, both positive (welds, debris) and negative (gaps, seams, etc.)
Antenna communications	
Ruggedized installation	Improve weldolet antenna plug design for more rugged installation (deployment/retrieval and retention)
Alternate configurations	
Video-Scout	Configure, deploy, and test (with new obstacle scripting) a video-only robot train (Video-Scout)
Pre-NDE run	Consider using the Video-Scout configuration to preinspect pipe run prior to NDE sensor run
Sensor evaluations	
RFEC data validity	Carry out baseline blind validity tests of SwRI RFEC sensor to validate system for commercial use
Field deployments	
Crew training	
Launcher and antenna ports	Ensure proper training to make sure all launchers/ports are usable at pressure
Postinstall cleanup	
Metal coupon	Ensure positive lock-on cut elliptical pipe coupon to avoid it dropping into pipe at launcher install
Metal shavings	Develop magnetic tool-on-a-stick to remove heavy launcher metal shavings left in pipe prior to use
Alternate sensing methods/devices	
Sensor development	
MFL sense/control modules	Build an operational MFL system with articulated sensor and separate electronics/control module
Design considerations	
Flux-shoe	Design of flux shoe for saturation and minimal (switchable?) magnetic drag is crucial
Rolling contact	Control standoff and use rolling contact to ensure and maintain stand-off to minimize frictional losses
Articulation	Design more rugged/fail-safe articulation elements of all sensors to avoid failure and nonretrievability

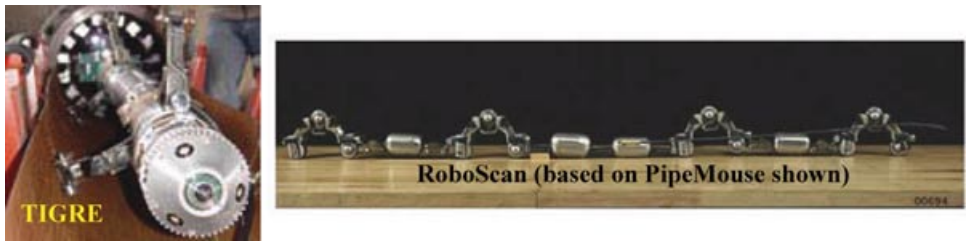

Figure 39. TIGRE and RoboScan: Additional prototype robot platforms under development for larger diameter unpiggable NG pipelines.

parts to an inspection company that will serve the national (and international) gas utility industry and its associated transmission and distribution companies. It is expected that a commercial prototype and actual inspection service should be available commercially by sometime late in 2009 to early 2010.

12. RELATED DEVELOPMENTS

In addition to the Explorer family of pipeline inspection robots, two additional systems are noteworthy as they target another NG delivery market segment: larger diameter pipelines at higher pressure with unpiggable pipe sections. These unpiggable sections are currently not inspectable using existing ILI technologies due to multiple factors, such as low flows/pressures, tight bends, diameter variations, plug valves, etc.

The DoE and DoT have both funded developments in this area, by developing (with both projects at different stages) both platforms (Leary, 2004; Schempf et al., 2005) and sensors (MFL; Larsen, 2005) for such pipeline markets. The TIGRE[8] platform (TIGRE Research Project, 2005; developed by Automatika, Inc.) is currently in a prototype and commercialization stage with additional pending field trials, and RoboScan (under development by Foster-Miller, Inc.)[9] has progressed to the preliminary design stage (Leary, 2004). Both these platforms are depicted in Figure 39.

13. COMMERCIAL PRIOR ART

In the area of pipe inspection and repair, multiple companies are currently active worldwide. Whether this be in water/sewer pipes,[10] oil/gas wells,[11] or even pipelines for hydrocarbon products,[12] multiple examples of successful commercial market segments and tailored remote systems exist, including reports by government entities on relevant studies, incidents, and technologies.[13] A complete and analytical survey paper may be called for in a future effort, but in the interim the reader is directed to the websites provided in footnotes 10–13.

ACKNOWLEDGMENTS

The development of the Explorer family of robots (X-I, X-II) was made possible by several contracts to CMU, primarily NETL/DoE (DE-FC26-01NT41155 and DE-FC26-04NT42264), secondarily NASA (Contract NCC5-223), and finally the North East Gas Association (NGA; Contracts

[8]http://www.automatika.com/products-tigre.htm; http://www.automatika.com/Collateral/Documents/English-US/PrjHome.rdm.htm

[9]Separately funded by DoE, NGA, & General Electric (GE); only completed design phase to date (2007).

[10]http://www.pearpoint.com; http://www.ka-te-system.com/html/homee.html; http://www.ulcrobotics.com/; http://www.blackhawk-pas.com; http://www.ais.fraunhofer.de/BAR/kurt.htm; http://www.inspector-systems.com/makro_plus.html; http://www.redzone.com/technology/robotics

[11]http://www.ariesind.com/gascam.html; http://www.advantica.biz/; http://www.bakerhughes.com/pmg; http://www.maurertechnology.com/Engr/Products/MFL.asp; http://www.welltractor.com/; http://www.bakerhughes.com/bot/service_tools/index.htm; http://www.invodane.com/feat_unpiggable.html

[12]http://www.foster-miller.com/t_robotics.htm; http://itrobotics.ath.cx/Products/Products.htm; http://www.nygas.org/M-2002-015.htm; http://www.tdwilliamson.com; http://www.roseninspection.net; http://www.gepower.com/prod_serv/serv/pipeline/en/index.htm; http://www.netl.doe.gov/technologies/oil-gas/publications/Status_Assessments/NT42264_Technology_Status_PipeExplorer_Nov04.pdf

[13]http://www.netl.doe.gov/scngo/Reference_Shelf/tsa/tsa-videoinspect-0202_1.PDF; http://www.netl.doe.gov/publications/press/2004/tl_oilgas_bbfa.html; http://www.netl.doe.gov/scngo/Natural_Gas/Projects_n/TD&S/T&D/T&D_C_41645RobotPlatform.html; http://primis.phmsa.dot.gov/matrix/PrjHome.rdm?prj=160; http://www.automatika.com/products-tigre.htm; http://www.netl.doe.gov/technologies/oil-gas/NaturalGas/Projects_n/TDS/TD/T&D_C_41645RobotPlatform.html; http://www.netl.doe.gov/technologies/oil-gas/publications/td/NT41645_FG033104.PDF; http://primis.phmsa.dot.gov/rd/techdemo.htm

M2000-004 and M2004-003). We wish to acknowledge the professional leadership to the program provided by DoE-NETL, in particular Rodney Anderson and Richard Baker. As part of the X-I field testing, we wish to thank KeySpan for their willingness and support in carrying out pressurized NG testing prior to field-trial deployment (D. D'Eletto and J. Vitelli). We wish to also acknowledge the X-I field-trial support of ConEdison, their excellent Yonkers field crew and management (P. Fowles and J. Sangirardi), as well as the RG&E R&D and field crew for their support during the medium-pressure steel demonstration in Brockport, New York. We wish to deeply thank and acknowledge the contribution and X-II field-trial support from the National Fuels, Inc., crew during the NG pressure testing (Henderson, Pennsylvania) and actual field trials in Brookville, Pennsylvania. The professional and unwavering integration support of all sensor modules by both SwRI and ATK are also worth acknowledging as contributing to the success of this program.

This paper discusses a program that was completed with cofunding support of the U.S. Department of Energy (DoE) under Award DE-FC26-01NT41155 and DE-FC26-04NT42264. However, any opinions, findings, conclusions, or recommendations expressed herein are those of the author(s) and do not necessarily reflect the views of the DoE.

REFERENCES

Burkhardt, G.L. (2007). Remote-field eddy current inspection system for small-diameter unpiggable pipelines. Technology Today, SwRI Quarterly Magazine, December.

Burkhardt, G.L., & Crouch, A.E. (2006, July). Remote-field eddy current sensing for inspection of gas distribution piping. In ASNT 15th Annual Research Symposium2006 Paper Summaries CD-ROM, Orlando, FL.

Burkhardt, G.L., & Crouch, A.E. (2007, March). Remote-field eddy current inspection system for small-diameter unpiggable pipelines. In Proceedings of the Pipeline Pigging and Integrity Management Conference, Houston, TX.

Burkhardt, G.L., Parvin, A.J., Peterson, R.H., Tennis, R.F., & Goyen, T.H. (2007, December). Remote-field eddy current inspection system for small-diameter unpiggable pipelines. In ASNT's International Chemical and Petroleum Industry Inspection Technology (ICPIIT) X Conference Paper Summaries Book, Houston, TX.

Cremer, C.D., & Kendrick, D.T. (1998, October). Case studies of uses of the pipe Explorer™ system. In Spectrum'98, International Conference on Decommissioning and Decontamination and on Nuclear and Hazardous Waste Management, Denver, CO.

Crouch, A.E., & Burkhardt, G.L. (2006, March). Development of sensor technology for integration into an inspection robot for unpiggable distribution mains. In Pipeline Pigging and Integrity Management Conference, Houston, TX.

DoE (2004). Phase I Report In-Pipe-Assessment Robot Platforms. http://www.netl.doe.gov/technologies/oil-gas/publications/Status_Assessments/NT42264_Technology_Status_PipeExplorer_Nov04.pdf.

DoT (1997). Guidance Manual for Operators of Small Natural Gas Systems. U.S. Department of Transportation, Research and Special Programs Administration.

DoT (2006). DoT-sponsored Sensor Evaluation. Internal Inspection Technology Demonstration Report website: http://primis.phmsa.dot.gov/rd/techdemo.htm.

Fisher, J.L. (1989). Remote-field eddy current inspection. In ASM handbook (pp. 195–201). Materials Park, OH: ASM International.

Hirose, S., Ohno, H., Mitsui, T., & Suyama, K. (1999, October). Design of in-pipe inspection vehicles for 25, 50, 150 mm diameter pipes. In Proceedings IEEE International Conference on Robotics & Automation, Yokohama, Japan (pp. 2309–2314).

Ilg, W., Berns, K., Cordes, S., Eberl, M., & Dillmann, R. (1997, September). A wheeled multijoint robot for autonomous sewer inspection. In Proceedings of III/RSJ IROS '97 (vol. 3, pp. 1687–1693).

Ives, G., Jr. (1998). Pipe ruptures. PipeLine & Gas Industry Journal, 83(9).

Larsen, P. (2005). Company website for multi-diameter MFL inspection tool used with TIGRE. http://www.invodane.com/feat_unpiggable.html.

Leary, W. (2004). Development of an inspection platform and a suite of sensors for assessing corrosion and mechanical damage on unpiggable transmission mains. DoE Final Project Report. Web sites include http://www.netl.doe.gov/technologies/oil-gas/NaturalGas/Projects_n/TDS/TD/T&D_C_41645RobotPlatform.html and http://www.netl.doe.gov/technologies/oil-gas/publications/td/NT41645_FG033104.PDF.

Paletta, L., Rome, E., & Pinz, A. (1999). Visual object detection for autonomous sewer robots. In Proceedings of 1999 IEEE/RSJ International Conference on Intelligent Robots and Systems (IROS '99) (vol. 2, pp. 1087–1093). Piscataway, NJ: IEEE Press.

Porter, C., & Pittard, G. (1999). Magnetic flux leakage technology for inspecting "live" gas-distribution mains (Tech. Rep. GRI-99/0199). Chicago, IL: GTI.

Roh, S.G., & Choi, H.R. (2005). Differential-drive in-pipe robot for moving inside urban gas pipelines. IEEE Transactions on Robotics, 21(1), 1–17.

Schempf, H. (2004). Method and system for moving equipment into and through an underground well. Pat.# 6,675,888.

Schempf, H., Mutschler, E., Crowley, W., Gavaert, A., Skoptsov, G., & Graham, T. (2003, September). Explorer: Untethered real-time gas main assessment robot system. In 1st International Workshop on Advances in Service Robotics, ASER'03, Bardolino, Italy.

Schempf, H., Mutschler, E., Crowley, W., Gavaert, A., Skoptsov, G., & Graham, T. (2005). Gas main robotic inspection system. U.S. Patent #6,917,176.

Schempf, H., Mutschler, E., Crowley, W., Goltsberg, V., & Chemel, B. (2003). GRISLEE: Gasmain repair & inspection system for live entry environments. CLAWAR '01 Special Issue, International Journal of Robotics Research, 22(3 and 4), 23–39.

Schempf, H., Mutschler, E., Crowley, W., Goltsberg, V., & Chemel, B. (2004). GRISLEE: Gasmain repair and inspection system for live entry environments. IEEE International Journal of Robotic Research, 37, 137–142.

Schempf, H., Mutschler, E., Goltsberg, V., & Chemel, B. (2001). Robotic repair system for live distribution gasmains. In Field and Service Robotics Conference, FSR 2001, Helsinki, Finland.

Schempf, H., & Vradis, G. (2004). Explorer: Long-range untethered real-time live gas main inspection system. In Natural Gas Technologies II Conference, Phoenix, AZ.

Staff Report. (2000). New optical methane detector improves gas leak surveys. PipeLine & Gas Industry Journal, 17, 17–21.

TIGRE Research Project. (2005). Co-Funded by DoT-PHMSA and NGA. Official public information release site: http://primis.phmsa.dot.gov/matrix/PrjHome.rdm?prj=160.